THE PENNSYLVANIA STATE UNIVERSITY
SCHREYER HONORS COLLEGE

DEPARTMENT OF BIOCHEMISTRY AND MOLECULAR BIOLOGY

ADDRESSING THE ROLE OF THE NOT4 E3 UBIQUITIN LIGASE DURING DNA DAMAGE-INDUCED DEGRADATION OF RNAPII IN BUDDING YEAST

LAURA MARGARET BEEBE
SPRING 2017

A thesis
submitted in partial fulfillment
of the requirements
for a baccalaureate degree
in Biochemistry and Molecular Biology
with honors in Biochemistry and Molecular Biology

Reviewed and approved* by the following:

Joseph C. Reese
Professor of Biochemistry and Molecular Biology
Thesis Supervisor
Honors Adviser

David S. Gilmour
Professor of Biochemistry and Molecular Biology
Committee Member, Department of Biochemistry and Molecular Biology

Scott Selleck
Department Head for Biochemistry and Molecular Biology

* Signatures are on file in the Schreyer Honors College.

ABSTRACT

Ccr4-Not is a multi-subunit gene regulatory protein complex that has been highly conserved in eukaryotes. Although first thought to solely act as a negative regulator for transcription, it has since been shown that Ccr4-Not is the major cytoplasmic deadenylase in yeast, and has subsequent functions in mRNA decay and control, RNA export, and translational repression. Most relevant to this study, the complex has been shown to have ubiquitylation activity—a process which can target proteins for degradation or modulate their activity. It has also been shown that ubiquitin proteases, such as Ubp3, are involved in transcription and are important to promoting cellular resistance to DNA damage. Connecting these two notions, previous work from the Reese laboratory has found that Not4, a subunit of Ccr4-Not, possesses a RING domain causing ubiquitin ligase activity involved in Rpb1 (the large subunit of RNA Polymerase II) turnover and degradation after DNA damage. In this work, we both verify this result and inform further study on whether Ccr4-Not plays a direct or indirect role in Rpb1 ubiquitylation and degradation, based on its genetic interactions with other enzymes in the transcription-coupled repair (TCR) and ubiquitin/proteasome pathways.

TABLE OF CONTENTS

LIST OF FIGURES v

ACKNOWLEDGEMENTS vi

Chapter 1 Introduction 1

1.1 RNAPII, Transcription, and Elongation 1

1.2 DNA Damage and Repair: An Overview 4

1.3 Transcription-Coupled Repair 6

1.4 The Ubiquitin/Proteasome Pathway 8

1.5 The Ccr4-Not Complex 10

1.6 Scope and Significance 13

Chapter 2 Materials And Methods 21

2.1 Materials 21

2.2 Generation of *DEF1* Knockout Cassette 21

2.3 Generation of *NOT4* Knockout Cassette 21

2.3.1 Isolation of Genomic DNA from JR1531 not4Δ::NATMX 21

2.3.2 Creation of NOT4 Knockout Cassette 23

2.3.3 Gel Purification of NOT4 Knockout Cassette 23

2.4 Deletion of *DEF1* in *not4*Δ Mutants; Deletion of *NOT4* in *rad26*Δ Mutants 24

2.4.1 Transformation 24

2.4.2 Verification by PCR 25

2.5 Creation of *NOT4/UBP3* Double Deletion Mutant via Mating and Dissection 26

2.5.1 Growth and Mating 26

2.5.2 Sporulation 26

2.5.3 Vivisection and Tetrad Dissection 26

2.5.4 Replica Plating 27

2.6 Spot Plating of NOT4 RING Domain Mutants 27

2.6.1 Measuring Synthetic Lethality of NOT4/DEF1 27

2.6.2 Measuring Mutant UV-Sensitivity Phenotypes 28

2.7 Spot Plating to Qualitatively Assay Mutant DNA Damage Phenotypes 28

2.8 UV Quantitative Assay of Mutant DNA Damage Phenotypes 29

2.9 Measuring Rpb1 Degradation During 4-NQO Treatment 30

2.9.1 Growth and Treatment of Cells 30

2.9.2 TCA Whole-Cell Extract Preparation 30

2.9.3 Standardization of Protein Loading Amounts via Coomassie Gel 31

2.9.4 SDS-PAGE and Protein Transfer 32

2.9.5 Western Blotting and Protein Detection Via ECL 33

2.9.6 Generating Rpb1 Degradation Plots 34

Chapter 3 Results 35

3.1 Selection and Verification of Yeast Mutants 35

3.2 Simultaneous *NOT4/DEF1* Deletion is Lethal in Yeast 38

3.3 *NOT4/UBP3* Double Mutants Show Greater Resistance to DNA Damage than *NOT4* Single Mutants 40

3.4 Rpb1 Degradation in Response to DNA Damage in *NOT4* Double Mutants 43

Chapter 4 Discussion 66

4.1 Not4 May Act Externally to A Known Pathway for DNA Damage-Induced Polyubiquitylation and Destruction of RNAPII 66

4.2 The Relationship of Not4 with Ubiquitin Proteases Acting on DNA Damage-Stalled RNAPII 69

4.3 Summary and Outlook 70

BIBLIOGRAPHY..73

LIST OF FIGURES

Figure 1.1: Initiation of Transcription by RNAPII 14

Figure 1.2: Modes of Rescue for Transcriptionally-Arrested RNAPII 15

Figure 1.3: The Nucleotide Excision Repair Pathway in Yeast 16

Figure 1.4: Mechanism for Polyubiquitylation of Proteins 17

Figure 1.5: Model for Degradation of DNA Damage-Independently Stalled RNAPII 18

Figure 1.6: The Ccr4-Not Complex 19

Figure 1.7: Ccr4-Not Rescues RNAPII From Arrest 20

Figure 3.1: Schematic of PCR-Mediated Gene Knockout in Yeast 47

Figure 3.2: Generation of PCR Knockout Cassettes 49

Figure 3.3: Primer Tests For Mutant Verification 51

Figure 3.4: The Budding Yeast Life Cycle 53

Figure 3.5: Tetrad Dissection Plate 54

Figure 3.6: Simultaneous *NOT4/DEF1* Deletion is Lethal in Yeast 55

Figure 3.7: Mutant Phenotype Response to DNA-Damaging Conditions 56

Figure 3.8: *not4*Δ Mutants are Temperature Sensitive 59

Figure 3.9: Mutant Survival Rates in Response to UV Radiation 60

Figure 3.10: The Not4 RING Domain is Important for Growth Under Stress Conditions 62

Figure 3.11: Mutant Rpb1 Degradation Phenotypes in Response to DNA Damage 63

Figure 4.1: Potential Models of Ccr4-Not Action During RNAPII Degradation in Response to DNA Damage 72

ACKNOWLEDGEMENTS

Thank you to Dr. Reese, and all the members of the Reese laboratory, for providing the scientific guidance and mentorship necessary to complete this project. Thank you especially to Diane Libert for her work in determining the importance of Not4 for RNAPII degradation during DNA damage. Additionally, thank you to the Penn State Eberly College of Science, which provided funding in support of my research.

Chapter 1

Introduction

1.1 RNAPII, Transcription, and Elongation

Transcription may be considered the central process within a cell, as it is the origin of information flow within the central dogma of molecular biology. Therefore, the regulation of transcription is of maximal importance in eukaryotic cells, in which the very structure of the genome must sometimes be modified to accommodate a desired pattern of gene expression. At the center of this critical process is RNA Polymerase (RNAP), the enzyme directly responsible for transcribing DNA to RNA.

There are three varieties of RNAP in eukaryotic cells: RNAPI, RNAPII, and RNAPIII. RNAPI and RNAPIII are responsible for transcribing genes that encode transfer RNA, ribosomal RNA, and various small RNAs. Here, we will focus on RNAPII, which transcribes all protein-coding genes, as well as snoRNA genes and some snRNA genes. RNAP in eukaryotes bears structural similarity to bacterial RNAP. However, there are two key differences that must be considered. First, while bacterial RNAP only requires a single initiation factor to begin transcription, eukaryotic RNAP requires the assembly of multiple general transcription factors at the gene promoter before transcription can begin. Second, eukaryotic RNAP must contend with DNA which has been packed into higher order chromatin structures, which are absent in prokaryotes (1).

Within the promoter of a gene to be transcribed, there exists a TATA sequence (or TATA box) located about twenty-five nucleotides upstream of the transcription start site. Here, the assembly of general transcription factors begins with TFIID (general transcription factor) via its TBP, or TATA-binding protein. The binding distorts the DNA, creating a "landmark" which portends the assembly of the transcription initiation complex, including several other transcription factors as well as RNAPII itself. After the initiation complex has formed, another general transcription factor, TFIIH, uses its DNA helicase activity to guide RNAPII onto the template strand. After a pause, TFIIH phosphorylates the C-terminal domain (CTD) of RNAPII, releasing it to begin transcription. This is followed by the release of the initiation complex, transcript elongation, and eventual termination (Figure 1.1) (1).

RNAPII then dissociates from the initiation factors, leaves the promoter, and forms a stable elongation complex to linearly transcribe DNA, perhaps via a Brownian ratchet mechanism (33, 25). As incoming, downstream DNA enters the elongation complex, it is unwound (forming a "transcription bubble"), allowing the template strand to contact the active site of RNAPII. Also attached to the active site via its 3' end, the growing RNA strand forms a hybrid duplex of about 8-9 base pairs with the template DNA (45). The transcription bubble is maintained throughout elongation, requiring continuous downstream DNA unwinding, separation of the nascent RNA strand from the template DNA, and reformation of the upstream DNA duplex (33). The RNA transcript grows via the nucleotide addition cycle, in which RNAPII selects a complementary ribonucleoside triphosphate (NTP), catalyzes the formation of a phosphodiester bond on the RNA 3'-end, and translocates along DNA and RNA to allow the next NTP to bind (58).

Elongating RNAPII exists in a constantly shifting biochemical equilibrium, associating with a rotating array of factors. General elongation factors, such as TFIIS, Elongin, TFIIF, and ELL, greatly improve the efficiency of RNAPII, which cannot smoothly transcribe DNA even under near-optimal conditions (46). For example, RNAPII frequently undergoes transient pausing and backtracking during elongation. These temporary stalling events can be triggered by specific DNA sequences, misincorporation events, or hairpins in the newly-formed RNA. Such an obstacle will initiate an "elemental pause," in which an interruption occurs within the RNAPII active site, fraying the 3' RNA end away from the DNA template. In the case of mismatch, RNAPII can backtrack by one step and then "proofread" the misincorporated base-pair, via its endonucleolytic activity.(33) In particular, TFIIS helps RNAPII to cleave its transcript in the backtracked position, enabling the enzyme to reestablish contact and resume transcription. However, TFIIS is not essential to yeast, and multiple parallel pathways exist to rescue the transiently stalled RNAPII. Post-translational modifications, such as ubiquitylation or CTD phosphorylation, plausibly allow the enzyme to "signal" a variety of transcriptional states and recruit the correct factors. (50)

Because RNAPII is very stably associated with DNA (as opposed to DNA polymerases, which interact dynamically with the DNA template), more permanent blocks to transcription cannot be easily bypassed. In response to DNA damage-induced lesions, reactivation of RNAPII by TFIIS is not effective. Instead, the cell must invoke repair pathways to remove the damage before transcription can proceed, ubiquitylate RNAPII as part of an alternate rescue mechanism, or, as a last resort, initiate ubiquitin-mediated degradation of RNAPII (Figure 1.2) (50).

1.2 DNA Damage and Repair: An Overview

Cells can incur DNA damage through a variety of endogenous and environmental sources. Reactive oxygen species and alkylating agents are poised to attack DNA after their intracellular formation as byproducts of metabolism. DNA itself, while highly stable, is subject to spontaneous hydrolytic deamination and depurination. Chemicals and radiation from the extracellular environment also damage DNA, leading, for example, to the formation of cyclobutane pyrimidine dimers. In total, the mammalian cell must contend with an estimated 10^4 – 10^5 DNA lesions per day. (51)

The structure of the DNA molecule is itself optimized for efficient repair. Its complementary strand essentially provides a backup of genetic information, facilitating easy repair of single-strand breaks. Double-strand breaks (DSBs) are more dangerous, as they threaten chromosomal integrity. However, end-joining mechanisms exist to repair such breaks. Nonhomologous end-joining, an “emergency solution” to DSBs, occurs commonly in mammalian cells. The two cut ends are simply rejoined by DNA ligation, resulting in the deletion or insertion of one or more nucleotides at the site of breakage. Homologous end-joining, more prevalent in microorganisms than in mammals, uses a collection of recombination proteins to repair DSBs—without mutation—with information from the undamaged sister chromosome in diploid cells (1).

DNA repair mechanisms are perhaps most relevant to organisms which are exposed to sunlight. Accordingly, molecular DNA repair was a process first described in 1949 when it was observed that visible light negated the DNA damaging effects of UV radiation in bacteria (photoreactivation) (24). Ten years later, it was shown that photoreactivating enzyme, or DNA photolyase, was responsible for the reversal due to its ability to convert light energy into

chemical energy (43). This allows the cell to repair UV-induced pyrimidine dimers. However, this is a nonessential enzyme which is by no means highly conserved, and many organisms (including humans) lack photolyase.

Of the mechanisms by which all eukaryotic cells contend with DNA damage, base excision repair (BER) and nucleotide excision repair (NER) are best understood. These processes take advantage of the redundant nature of double stranded DNA, by first removing the damage and then using the complementary strand as a template for repair. BER is the more limited form of the two, employing a two-step process. A DNA glycosylase first removes the damaged base, and then AP (apurinic/apyrimidinic) endonucleases excise the abasic sugar (45). Because the DNA glycosylases must interact closely with the lesion itself in order to catalyze its removal, BER only operates on a small range of substrates. Damaged DNA bases can be identified by their structure: every possible DNA deamination reaction yields an unnatural base, which is readily detected by DNA glycosylase (1). Thus, DNA is well protected from spontaneous alterations to the genetic code. Some safeguards work better than others, however. One harmless mutation is the spontaneous conversion from cytosine to uracil, via deamination. This is quickly reversed by uracil DNA glycosylase. A more deleterious change, by contrast, involves the deamination of methylated cytosine, which yields thymine mismatched to guanine. While designated DNA glycosylase recognizes this mismatch and removes the thymine, it does not seem to be very effective— only 3% of cytosine in human DNA is methylated, but mutations in these bases make up about 30% of single-base mutations seen in inherited diseases (1).

NER is a ubiquitous procedure which has been conserved among essentially all types of cells. Its “cut and patch” mechanism was first observed in *E. coli*, when cells irradiated with UV light were shown to excise the subsequently formed pyrimidine dimers and then display short

stretches of new DNA synthesis (16). Despite being conserved across organisms, NER is a highly complex process, requiring a large system of enzymes. In contrast with BER, the enzyme system hydrolyzes phosphodiester bonds on either side of the DNA lesion, generating an oligonucleotide which contains the damage rather than just removing a damaged base. Both the position and distance between the two hydrolysis sites is precisely defined in prokaryotes and eukaryotes. (Prokaryotes generate oligomers of 12 to 13 nucleotides, while eukaryotes generate oligomers that are 27 to 29 nucleotides in length). The reaction proceeds via a nuclease that is unique to DNA repair, termed excision endonuclease, or excinuclease, to keep it distinct from endonucleases and exonucleases used for other intracellular functions (45). After the oligonucleotide is excised, it is released from the duplex, and DNA polymerase plus DNA ligase work together to fill in new nucleotides and then seal the nick.

1.3 Transcription-Coupled Repair

The general NER pathway can be subdivided into global genome NER (GG-NER) and transcription-coupled NER, or transcription-coupled repair (TCR) (Figure 1.3). During GG-NER, the entire genome is screened for helix distortions, irrespective of chromatin structure or transcription status (4, 32). In general, this mechanism functions by "flipping out" the damaged bases, exposing them to solvent, before initiating repair. In yeast, this has been shown *in vitro* to occur when Rad4 and Rad23 ("Rad" signifies *rad*iation sensitive) form a stable complex with UV-irradiated DNA, inserting a β-hairpin through the DNA duplex (36). More relevant to this work, however, TCR is a process which is activated specifically when RNAPII is stalled by a

DNA lesion. DNA damage is thus sensed indirectly, in contrast to GG-NER, as there are no known “translesion” RNA Polymerases which can bypass damage without stalling (32).

The basic method of TCR is relatively well-understood in bacteria as a means of detecting cyclobutane pyrimidine dimers (CPDs) with higher sensitivity than during GG-NER (16). As RNAP stalls on a damaged gene, it blocks UvrA and UvrB (bacterial NER factors) from accessing the lesion. The transcription factor Mfd provides a means of releasing RNAP, perhaps by applying torque via its ATPase activity (40). Mfd also has a UvrB homology module, enabling it to recruit UvrA (which subsequently recruits UvrB) and thus repair the damage via the same pathway as in GG-NER. It has been shown that *Mfd* bacterial mutants are viable and only slightly more UV-sensitive. Hence, it seems that in this instance, TCR functions as a more precise backup to GG-NER, enabling rapid repair as damage is detected by RNAP (16).

CPD-stalled RNAPII in eukaryotes similarly prevents NER machinery from repairing DNA damage (it covers about 35 nucleotides in total (55), but exactly how RNAPII is removed is not fully understood. RNAPII backtracking, which also occurs regularly during proofreading and at normal pauses in transcription, may be the primary means of exposing the site of damage (47). But even so, it is not well understood what factors initiate backtracking or lead to the assembly of the repair complex. RNAPII may also dissociate from DNA, or, as a last resort, be targeted for degradation (33, 50).

Rad26 was the first eukaryotic protein found to be selectively involved in TCR (57). Its deletion yields yeast which are viable and have no significant growth defect, and, interestingly, show relatively uninhibited repair of transcribed DNA strands. This phenotype either suggests

that Rad26 is not involved in removing stalled RNAPII from a gene, but rather in some other aspect of NER, or that the cell has other ways to remove RNAPII.

It was later shown that Rad26 in fact forms a complex with Def1 (RNAP *de*gradation *f*actor), and that these two proteins work in tandem to regulate the "last resort" degradation of RNAP in response to arrest caused by DNA damage (60). Cells lacking Rad26 were shown to degrade RNAP faster than in the wild type, with Def1 no longer necessary for degradation. Contrastingly, cells without Def1 lacked RNAPII degradation altogether. This suggests that the role of Rad26 may be to pause the degradation of RNAP, permitting time for repair, and that Def1 is required to remove the inhibition.

1.4 The Ubiquitin/Proteasome Pathway

Ubiquitylation, the covalent ligation of ubiquitin to intracellular proteins, is an essential process which can target proteins for degradation by the proteasome (polyubiquitylation) or modulate their activity (monoubiquitylation). Monoubiquitylation also can alter a protein's function by marking it for interaction with other proteins. Ubiquitin-mediated degradation is necessary to regulate many processes in the cell, such as the cell-cycle, signal transduction, transcription, and endocytosis. The ubiquitin system operates through three separate classes enzymes: E1, E2, and E3 (Figure 1.4). In yeast, only one E1, or ubiquitin-activating enzyme, exists. In contrast, there are several E2s, or ubiquitin-conjugating enzymes, and a huge number of E3s, or ubiquitin ligases. After E1 activates ubiquitin, E2 and E3 enzymes form a complex in order to recognize and ubiquitylate their protein substrate (19, 49).

Studies on the Ubc5/Rsp5 (E2/E3) pair reveal that this complex is necessary for RNAPII degradation in yeast, providing interesting mechanistic details with respect to both the activity of the polymerase and its recognition by the E2/E3. It was shown that ubiquitylation of RNAPII by Rsp5 occurs necessarily on just two specific lysine residues, K330 and K695, both found on Rbp1 (the large subunit of RNAPII). The ubiquitylation likely occurs via two distinct events, with two E2/E3 complexes forming on RNAPII. This suggests that the location of the ubiquitylation sites is functionally important, which is supported by the observation that Ubc5 preferentially binds the elongating form of RNAPII *in vitro* (49).

However, it was later shown that Elc1 (Elongin Cullin) forms part of a ubiquitin-ligase also needed for RNAPII degradation; i.e., Ubc5/Rsp5 are not the only factors implicated in this process (42). In fact, Elc1 and Rsp5 seem to work as part of a sequential, two-step mechanism. Rsp5 acts first, adding mono-ubiquitin without triggering proteolysis. Sensing mono-ubiquitin, Elc1/Cul3 then produces and attaches a ubiquitin chain, promoting degradation. Thus, RNAPII can only be degraded as a result of cooperation between distinct, stepwise-acting ubiquitin ligases (18).

Interestingly, the Elc1/Cul3 degradation pathway may be active only when RNAPII is stalled by DNA damage. Recent evidence has shown that in instances where RNAPII is stalled independently of DNA damage (such as when elongation is not functional), degradation of RNAPII may proceed via an overlapping, but distinct pathway (22, Figure 1.5). The branch point could be Def1, which has been shown to recruit the Elongin-Cullin E3 ligase via a ubiquitin homology domain (59). The key difference between these proposed pathways rests in whether the cell recruits repair factors (like Rad26) to the DNA, which could be necessary for Def1 to enlist Elc1/Cul3.

In addition to enzymes which ubiquitylate other proteins, cells also have ubiquitin proteases, whose role is to remove ubiquitin. Ubp3 is one of eighteen predicted ubiquitin proteases in budding yeast, and has an important role in regulating the cell's DNA damage response. Upb3 forms a complex with Bre5 *in vivo*, a protein which contains a nuclear transport factor 2 domain (found to interact with Ubp3), a putative SH3 binding domain, and an RNA recognition motif. Most importantly, however, Upb3 has been shown to act on both mono- and polyubiquitylated RNAPII in yeast. It was additionally purified *in vitro* with RNAPII and Def1, along with the elongation factors Spt5 and TFIIF. Moreover, *ubp3* cells have higher levels of ubiquitylated RNAPII *in vivo*, which are degraded faster after UV irradiation.(28) Hence, Ubp3 provides an important counterbalance in the cell's decision of whether to degrade RNAPII during instances of DNA damage. This supports the idea that degradation of RNAPII is a "last resort" response, occurring only when swift repair of a transcription-stalling lesion is not possible.

1.5 The Ccr4-Not Complex

Ccr4-Not is a multi-subunit gene regulatory protein complex that has been highly conserved in eukaryotes. Although first thought to solely act as a negative regulator for transcription, it has since been shown that Ccr4-Not is the major cytoplasmic deadenylase in yeast, and has subsequent functions in mRNA decay and control, RNA export, and translational repression (35). The complex is made up of nine core subunits (Ccr4, Caf1, Caf40, Caf130, and Not 1-5) which each have precise and only partially overlapping functions, generating distinct

mutant phenotypes with deletion of different subunits (Figure 1.6). It is not well understood why these functionally separate subunits aggregate in a single complex, although one possible explanation is that Ccr4-Not may operate as a "chaperone platform" to assemble other multi-subunit complexes.(6)

The Ccr4-Not complex may be described as a "birth to death" regulator of gene expression, having been shown to play a role in both transcription of mRNA and in its eventual degradation (35). Importantly, the complex is likely to be part of the eukaryotic cell's response to stress, as it is well equipped to elicit a fast change in all levels of gene expression after the cell receives transient stress signals. In effect, the complex can exert a high degree of control over whether a gene product is translated or marked for degradation. This is strongly evident, for example, in the role of Ccr4-Not in mRNA deadenylation. Puf5, an mRNA binding protein in yeast, has been shown to selectively recruit Ccr4-Not to mRNAs in order to mediate their decay via Caf1 and Ccr4 deadenylation activity (35). In *puf5* mutants, cells show a higher sensitivity to stress conditions (38). Furthermore, there are multiple members of the PUF protein family which immunoprecipitate with the same mRNA, and Caf1 and Ccr4 also have different roles in the cell that are independent of Puf5 (35). All of this suggests a dynamic role of Ccr4-Not that is dependent on cell conditions.

Critical to this study, however, Ccr4-Not plays an important role in transcription, having been established in the Reese laboratory as a positive elongation factor for RNAPII (Figure 1.7). It interacts directly with RNAPII during elongation, and can "re-start" an RNAPII which has backtracked or been arrested *in vitro*. The complex thus directly regulates transcription, both through interactions with RNAPII itself and by binding with functional RNAPII elongation complexes. What is perhaps most interesting about Ccr4-Not's transcriptional role is that there

is no detectable change in elongation unless RNAPII is arrested. Therefore, the role of Ccr4-Not in elongation seems to revolve around resuming, rather than continuing transcription. (27)

Additionally, Ccr4-Not possesses ubiquitylation activity, and has been shown to target nuclear proteins, via its Not4 subunit. Not4 contains a Really Interesting New Gene (RING) domain, enabling its function as an E3 ubiquitin ligase (8). This activity allows it to regulate levels of histone H3 K4 trimethylation (H3 K4me3), by targeting Jhd2, the single H3 K4me3-specific histone demethylase in yeast. Indeed, it was shown that Not4 mutants lacking a RING domain were unable to regulate H3 K4me3 and Jhd2 turnover (33). Not4 may polyubiquitylate Jhd2 during transcription, as Ccr4-Not interacts with elongating RNAPII. Importantly, Not4 is known to have other nuclear substrates which could also be plausibly targeted during transcription, such as cyclin C (a subunit of mediator, an important transcriptional coactivator), which undergoes Not4-dependent stress-induced destruction. (41)

The knowledge that Ccr4-Not interacts intimately with stalled RNAPII logically prompts a consideration of its role in TCR. Since it is known that DNA lesions can only be repaired when stalled RNAPII is removed from the site of transcription, what role might Ccr4-Not play in facilitating this repair? The known role of ubiquitin-mediated degradation of RNAPII, coupled with the activity of regulatory ubiquitin proteases, also bodes increased significance for Ccr4-Not. Previous work from the Reese laboratory has found that the ubiquitin ligase RING domain of Not4 is involved in Rbp1 (the large subunit of RNA Polymerase II) turnover and degradation after DNA damage (30). The aim of this study is to attempt to both verify this result and determine if Ccr4-Not plays a direct or indirect role in Rbp1 ubiquitylation and degradation.

1.6 Scope and Significance

Stress response in humans activates repair pathways that can eliminate accumulated genetic damage. Left unchecked, lesions in DNA can eventually lead to diseases like cancer (through the activation of oncogenes or the inactivation of tumor suppressor genes, for example). DNA damage may also halt transcription, upsetting cellular homeostasis or even causing premature cell death (32). In addition, three rare human hereditary disorders—xeroderma pigmentosum, Cockayne's syndrome, and trichothio dystrophy—show defects in essential TCR machinery. This can have debilitating consequences, especially in the case of Cockayne's syndrome or trichothio dystrophy, whose patients show severe developmental defects (15). Many of the defective human enzymes in these diseases have direct homologs in yeast. Understanding the DNA damage repair pathway will allow researchers to address its alterations, ultimately leading to the prevention and treatment of ailments caused by accumulated mutations.

Figure 1.1: Initiation of Transcription by RNAPII

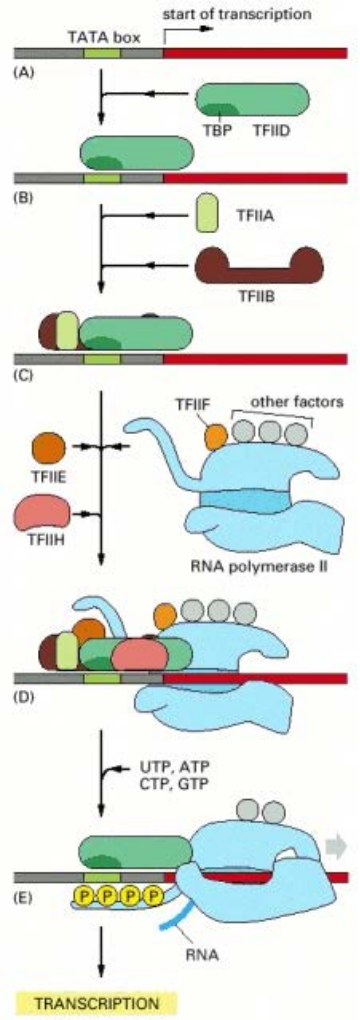

Figure 1.1: Initiation of Transcription by RNAPII. Taken from (1). Initiation of transcription begins with the assembly of general transcription factors at the TATA box (located within the promoter of a gene of interest). TFIID, or general transcription factor, binds first, creating a small distortion in the DNA which signals the recruitment of the full initiation complex. TFIIH then uses its helicase activity to guide RNAPII onto the template strand, and phosphorylates the enzyme's CTD to initiate transcription.

Figure 1.2: Modes of Rescue for Transcriptionally-Arrested RNAPII

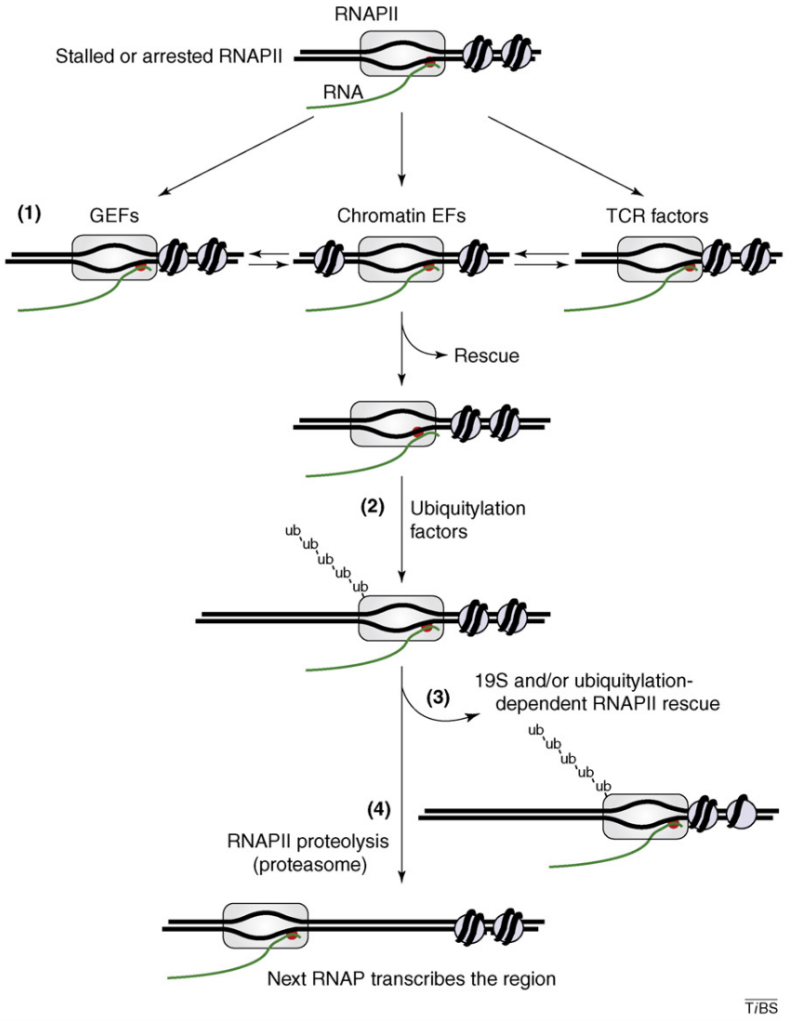

Figure 1.2: Modes of Rescue for Transcriptionally-Arrested RNAPII. Taken from (50). Rescue of stalled RNAPII is mediated by the TFIIS elongation factor, or by TCR factors like Rad26 if the stalling is caused by a lesion in the DNA. The 19S proteasome may also play some degradation-independent role in rescuing RNAPII and promoting elongation. If rescue is impossible, RNAPII is polyubiquitylated and degraded as a "last resort" response.

Figure 1.3: The Nucleotide Excision Repair Pathway in Yeast

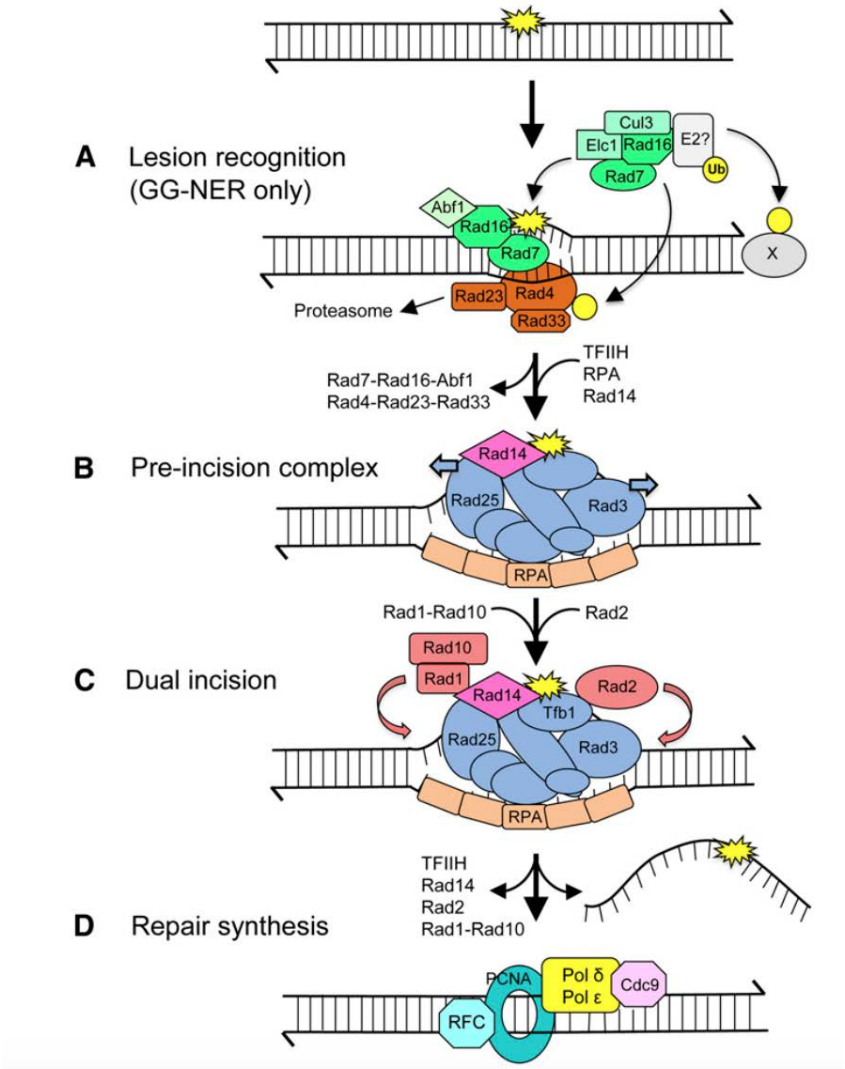

Figure 1.3: The Nucleotide Excision Repair Pathway in Yeast. Taken from (4). (A) depicts global-genome NER, in which the entire genome is scanned for helix distortions. This occurs when Rad4 and Rad23 form a stable complex with UV-irradiated DNA, inserting a beta-hairpin through the DNA duplex. (B, C, D) depict features of transcription-coupled NER, in which phosphodiester bonds on either side of the DNA lesion are hydrolyzed to excise the damage.

Figure 1.4: Mechanism for Polyubiquitylation of Proteins

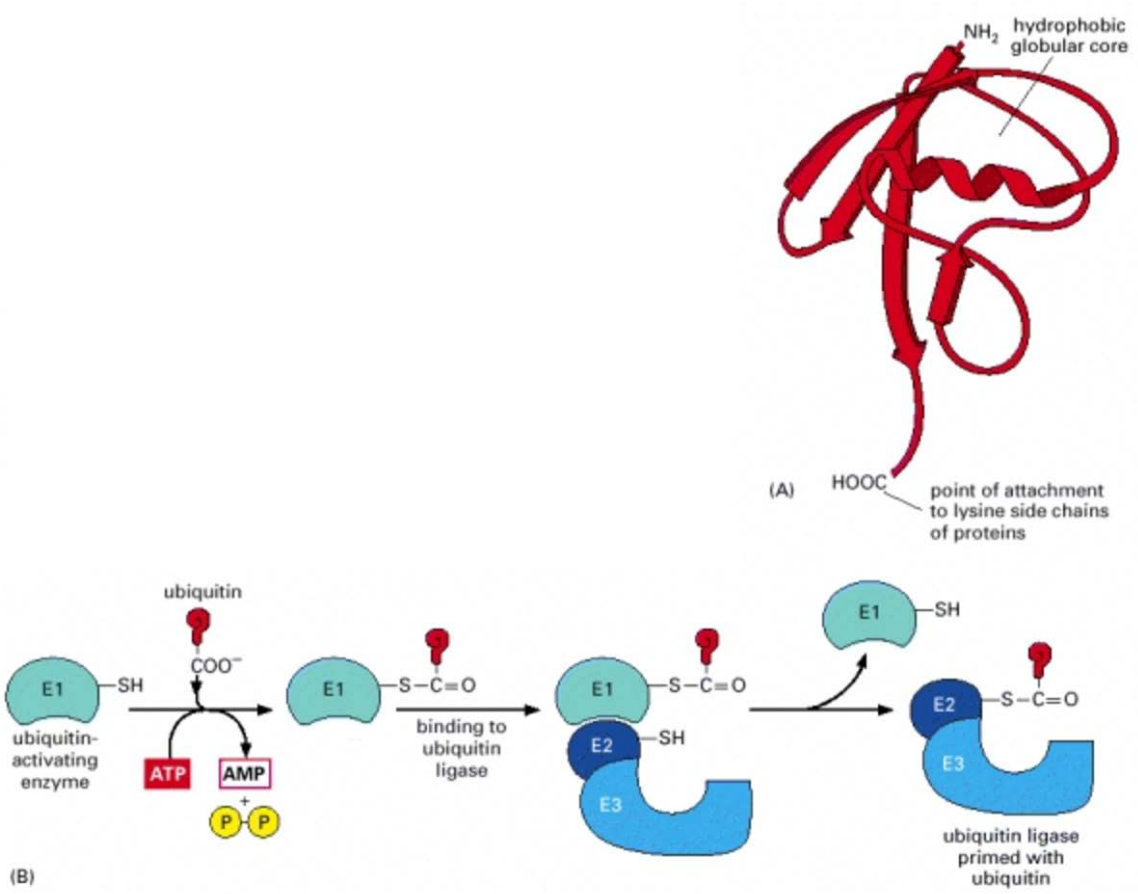

Figure 1.4: Mechanism for Polyubiquitylation of Proteins. Taken from (1). The ubiquitin-activating enzyme, or E1 protein, binds to ubiquitin via the formation of an ATP-dependent high-energy thioester linkage. Ubiquitin is then transferred to an E2 ubiquitin-conjugating enzyme, facilitating protein ubiquitylation via an E3 ubiquitin ligase.

Figure 1.5: Model for Degradation of DNA Damage-Independently Stalled RNAPII

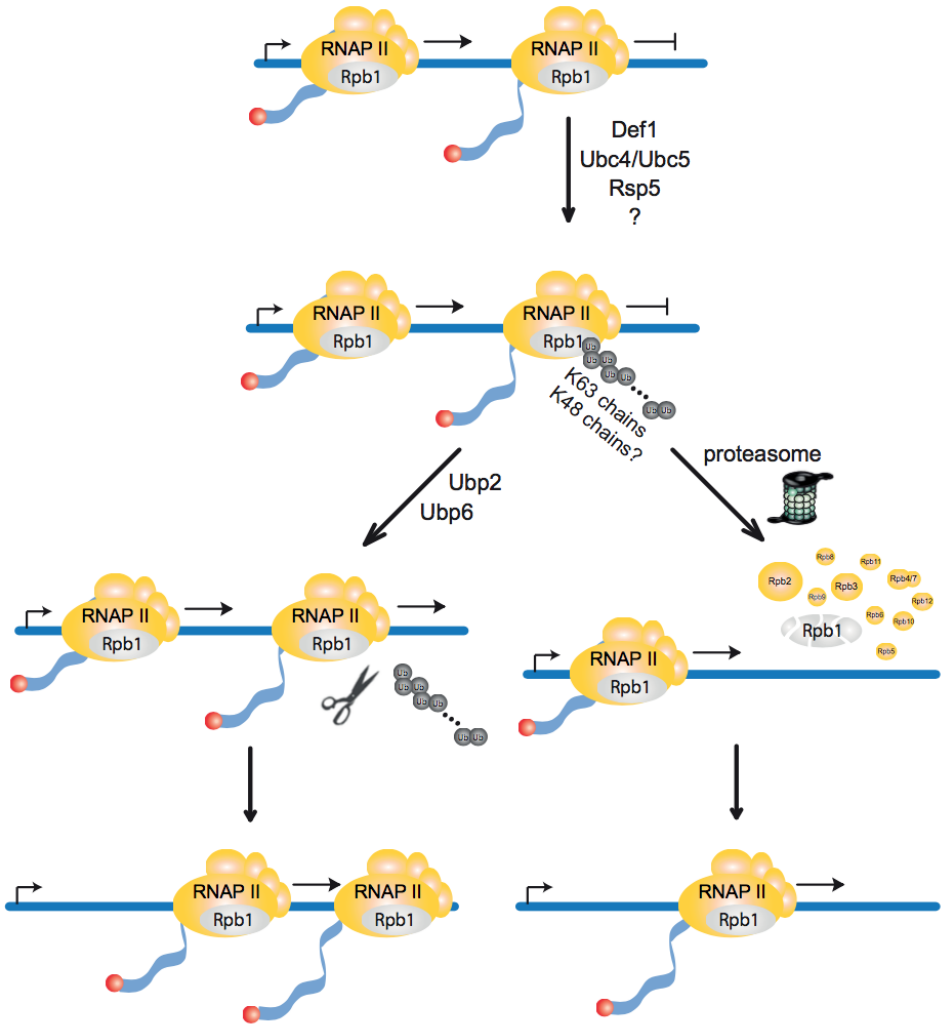

Figure 1.5: Model for Degradation of DNA Damage-Independently Stalled RNAPII. Taken from (22). Polyubiquitylation of stalled RNAPII is mediated by the actions of Def1, as well as E2 ligases Ubc4 and Ubc5 and E3 ligase Rsp5. Degradation is a "last resort" response; if the stalling can be ameliorated, RNAPII is deubiquitylated and transcription resumes.

Figure 1.6: The Ccr4-Not Complex

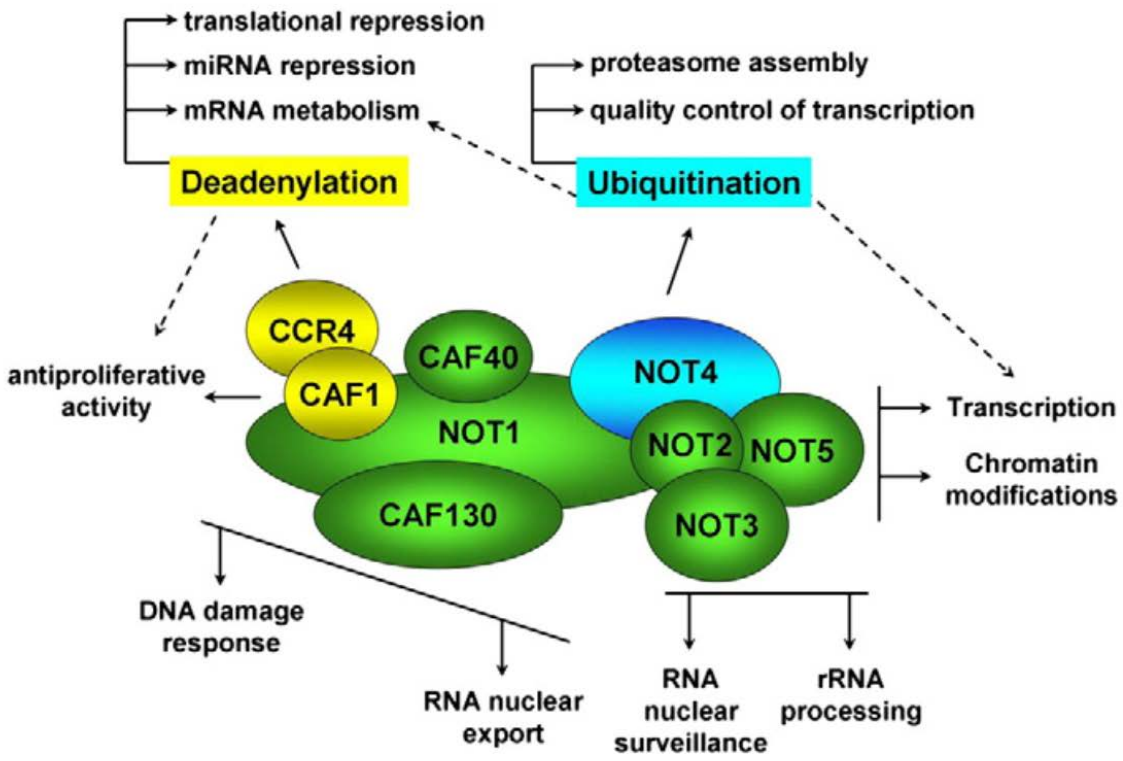

Figure 1.6: The Ccr4-Not Complex. Taken from (6). Ccr4-Not is a multi-subunit gene regulatory complex that is highly conserved in eukaryotes. This study mainly focuses on the ubiquitylation activity of Not4, a RING-containing E3 ligase. Ccr4-Not is a "birth to death" regulator of mRNA, playing a role in both mRNA transcription and its eventual degradation. The complex is thus well-endowed to play an important role in the eukaryotic cell's response to stress, as it can elicit rapid changes in gene expression in response to stress signals.

Figure 1.7: Ccr4-Not Rescues RNAPII From Arrest

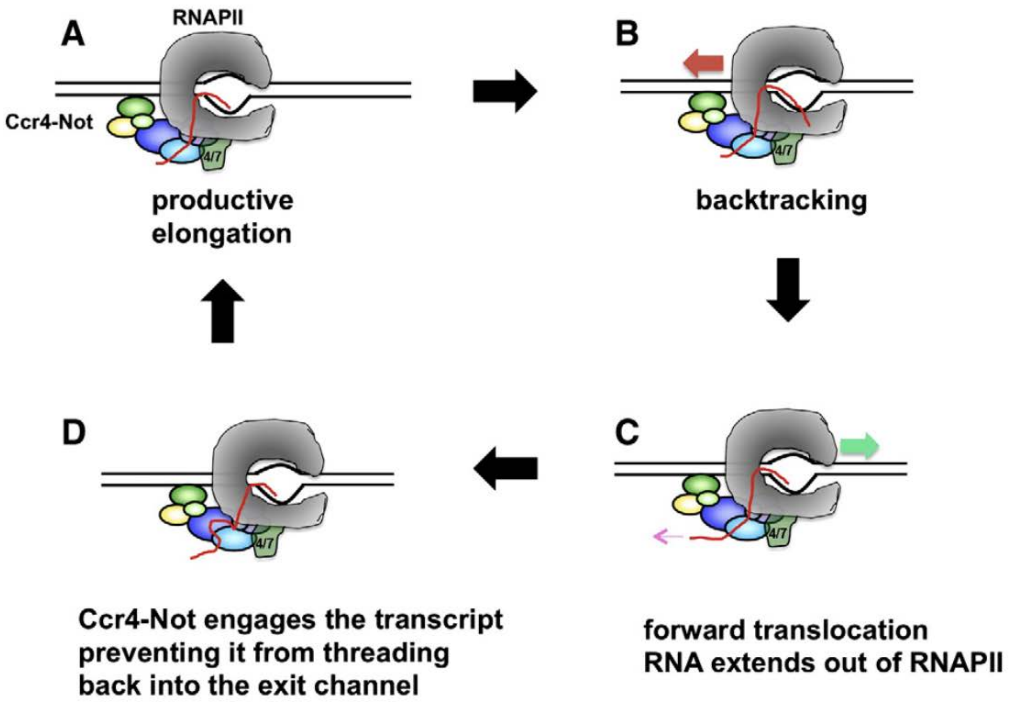

Figure 1.7: Ccr4-Not rescues RNAPII from arrest. Taken from (41). When RNAPII encounters a block in transcription, the enzyme may pause or backtrack. Ccr4-Not interacts closely with the stalled polymerase, preventing the transcript from reentering the exit channel. Knowledge that the Ccr4-Not complex has a close association with stalled RNAPII, in concert with its known ubiquitylation activity via the Not4 subunit, prompts consideration of the complex's role in transcription-coupled repair.

Chapter 2

Materials And Methods

2.1 Materials

Standard materials were used for all experiments. Optical density (OD) measurements were taken using a Thermo Scientific Genesys 20. YPD media contained 20 g/L bacto-peptone, 10 g/L yeast extract, 20 mg/L adenine sulfate, and 2% dextrose. Minimal drop out media contained 6.8 g/L yeast nitrogen base with ammonium sulfate, 10% 10X amino acid mix, and 2% dextrose.

2.2 Generation of *DEF1* Knockout Cassette

The pRS403 plasmid, along with a set of *DEF1*-specific knockout primers, was used to generate the *DEF1::HIS3* knockout cassette via PCR (5; also see section 3.1). The generated product was purified via ethanol precipitation. 3 µl of cassette (combined with 2 µl of dye) was visualized on a 1.2% agarose gel with ethidium bromide (EtBr) alongside 5 µl of 1 kb GeneRuler ™ DNA ladder.

2.3 Generation of *NOT4* Knockout Cassette

2.3.1 Isolation of Genomic DNA from JR1531 not4Δ::NATMX

The following genomic DNA preparation was used to ensure isolation of higher quality DNA, due to the large size of the fragment of interest. Cells were grown overnight to saturation

in 5 ml YPD. The next day, the yeast were allowed to settle for 20-30 minutes and transferred to a 1.7 ml microfuge tube with a cut P1000 tip. After centrifuging for 30 seconds, the supernatant was removed and resuspended in 1 ml of wash solution (1 M sorbitol and 0.1 M EDTA). The sample was centrifuged for 1 min. at 8000 rpm, and the supernatant was removed by aspiration.

The pellet was resuspended in 400 µl of digestion solution (0.96 M sorbitol, 0.1 M EDTA, and 14 mM 2-mercaptoethanol). 10 µl of 10 mg/ml zymolyase solution was added and mixed by vortexing gently. The sample was placed at 30° C for 30 minutes, and then centrifuged for 15 seconds. Using an aspirator, the supernatant was removed, and the pellet was resuspended in 370 µl TE. 120 µl of lysis solution (1.2 ml 0.5 M EDTA ph 8, 3 ml 1 M Tris-HCl pH 10, 1.2 ml 10% SDS) was added. The sample was vortexed hard for ten seconds and then placed at 65-68° C for 30 minutes. 110 µl of 5M potassium acetate was added, and the sample was vortexed and then placed on ice for 60 minutes. 450 µl of supernatant was recovered after centrifuging at full speed for 15 min. 1 ml of room temperature ethanol was added and mixed well, and the sample was allowed to stand at room temperature for 10 minutes. The sample was centrifuged for 5 minutes and supernatant was again removed using an aspirator. 350 µl TE containing 50 µg RNAse A was added, and the tube was vortexed and placed at 37° C. Vortexing continued every 5-10 minutes until the pellet was broken up. Resuspension occurred overnight at 4° C until the next morning, when the sample was placed at 37° C for 20 minutes.

The sample was centrifuged for 15 minutes at the highest speed, and 300 µl of the supernatant was transferred to a fresh tube. 300 µl of isopropanol was added and gently mixed, and DNA was allowed to precipitate for ten minutes at room temperature before centrifuging at full speed for five minutes. The supernatant was removed via aspiration, and the sample was allowed to air-dry. The new pellet was resuspended in 100 µl TE and stored at -20° C.

2.3.2 Creation of NOT4 Knockout Cassette

The isolated gDNA, along with a set of *NOT4*-specific knockout primers, was used to generate the *NOT4::NATMX* knockout cassette via PCR. 5 µl of DMSO was added to the reaction per µl of DNA template, as the *NATMX* cassette is GC-rich. 10 µl of product was removed from the aggregated PCR reactions for visualization on an agarose gel, in order to verify generation of the cassette. 3 µl of cassette (combined with 2 µl of dye) was visualized on a 1.2% agarose gel with ethidium bromide (EtBr) alongside 5 µl of 1 kb GeneRuler ™ DNA ladder.

2.3.3 Gel Purification of NOT4 Knockout Cassette

30 µl 3M NaOAc and 750 µl ethanol was added to the remaining PCR reactions (totaling about 290 µl), and the product was precipitated with ethanol. The pellet was resuspended in 50 µl TE to prepare for gel purification. DNA was loaded into 5 wells of a 1.2 % low-melting agarose gel, which was run at room temperature in 1.5X TAE. The bands were then excised from the gel (using a UV box for visualization) with a clean razor blade. After briefly centrifuging the gel slice, a 1/100 volume of 5M NaCl was added. The slice was melted at 68 – 70° C and vortexed well. Pre-warmed STE (pH 8.0) was added up to 500 µl. The sample was quickly vortexed, placed at 42° C for ten minutes, and then on crushed dry ice for 15 – 20 minutes. After freezing, the tube was placed in a 42° C water block until the contents started to melt. The tube was removed and vortexed hard at room temperature until the contents were fully melted, and then centrifuged for 8 minutes at full speed. Supernatant was recovered and transferred to a fresh tube, where an equal volume of CIAA was added. The tube was vortexed

for 15 seconds, centrifuged for 2 minutes at room temperature, and the upper aqueous layer was transferred to a fresh tube. A 1/10 volume NaoAc and 2 volumes cold ethanol were added, and the sample was precipitated for 15 minutes on dry ice. The sample was centrifuged for 10 minutes at full speed, the supernatant was removed, and 1 ml of 70% ethanol was added. After centrifuging again for 3 minutes, the supernatant was removed and the sample was allowed to dry. The pellet was resuspended vigorously in 0.1X TE and centrifuged for five minutes at full speed. The supernatant was recovered and transferred to a fresh tube. 1/10 of the total was run on a 1.2% agarose gel next to 5 µl of 1 kb GeneRuler ™ DNA ladder.

2.4 Deletion of *DEF1* in *not4*Δ Mutants; Deletion of *NOT4* in *rad26*Δ Mutants

2.4.1 Transformation

The newly generated *NOT4::NATMX* cassette was transformed into JR1697 and JR1698, the BY4741 and BY4742 versions of the *rad26*Δ::*KANMX* single deletion mutant. Before transforming with the *DEF1::HIS3* cassette, the JR1531 *not4*Δ strain was first transformed with a *URA3*-marked plasmid containing a wild type copy of *NOT4* (pDPM9-pRS416-NOT4-HA).

Cells to be transformed were grown 5 ml overnight cultures (YPD for *rad26*Δ strains, -URA for *not4*Δ containing the *URA3*-marked plasmid). The next day, 50 ml of culture was inoculated in order to achieve an OD600 of 1.0 after reaching log-phase growth. The cells were harvested via centrifugation, washed, and resuspended with LioAc-TE.

1-3 µg plasmid/fragment DNA, 50 µg salmon sperm carrier DNA, and 50 µl of cell suspension were combined in a microfuge tube. 300 µl PLATE solution (1 ml 10X LioAc, 1 ml 10X TE, and 8 ml 50% PEG) was added immediately, and the tubes were vortexed on medium

speed for ten seconds. The tubes were incubated on a roller-drum at 30° C for 30 minutes, and then placed at 42° C for 15 minutes. For *NATMX* selection, the cells were centrifuged at 8K for two minutes in a microfuge and then resuspended in 1 ml YPD for a 4-5 hour incubation period at 30° C. The cells were then plated on 100 µg/ml Clonat plates. For –HIS/URA selection, the cells were centrifuged at 8K for 2 minutes in a microfuge resuspended in 500 µl of sterile TE. They were then immediately plated on –HIS/-URA media.

2.4.2 Verification by PCR

Genomic DNA was isolated from the transformed colonies grown on selective media. A pin-head amount of yeast was taken from chosen colonies and resuspended in 50 µl digestion buffer (800 µl 1.2 M sorbitol, 200 µl 0.5 M EDTA, 1 µl 2-mercaptoethanol, 40 µl 10 mg/ml Zymolyase). Samples were incubated in digestion buffer at 30° C for 30 minutes. The tubes were then centrifuged at 5,000 rpm for 3 minutes, and supernatant liquid was removed by aspiration. The pellet was resuspended in 120 µl TE by vortexing. 200 µl glass beads were added along with 120 µl phenol-chloroform isoamyl alcohol (PCIAA), and the tubes were vortexed for one minute at the highest speed. After vortexing, the samples were centrifuged at 14,000 rpm for 5 minutes, and 75 µl of the supernatant was moved to a fresh tube. 80 µl CIAA was added once, and tubes were vortexed on high for ten seconds before centrifuging at the highest speed for two minutes. 40 µl of supernatant was transferred to a fresh tube and saved at -20° C. 1 µl of genomic DNA was used in PCR diagnostic tests, using both ORF diagnostic primers and gene-specific/marker-specific diagnostic primers. PCR products were visualized with EtBr on a 1.2% agarose gel.

2.5 Creation of *NOT4/UBP3* Double Deletion Mutant via Mating and Dissection

2.5.1 Growth and Mating

Single *not4*Δ (JR1531, *NOT4::NATMX*) and *ubp3*Δ (JR1700, *UBP3::KANMX*) yeast mutants were grown individually in YPD overnight. The next day, a 5 ml culture containing both strains was prepared so that the final OD600 of each strain was approximately 0.2. The cells were left to grow and mate at 30° C for 4-6 hours, and then plated onto solid YPD media containing Clonat and G418 (to select for diploids). Single colonies were allowed to form for about 2 days, and 2-3 individual colonies were re-plated and allowed to grow on selective media. The cells were then transferred to YPD.

2.5.2 Sporulation

Cells were taken from freshly grown YPD plates and moved onto newly prepared GNA presporulation plates (5% dextrose, 3% bacto-peptone, 1% yeast extract, 2% bacto-agar) to grow for 24 hours at 30° C. A pin-head quantity of cells was then transferred to 3 ml liquid sporulation medium (1 g potassium acetate, 1 ml 20% sterile-filtered raffinose, and 100 ml ddH2O at pH 7.0) and incubated overnight at 25° C, followed by 4-5 days at 30° C.

2.5.3 Vivisection and Tetrad Dissection

75 µls of sporulation culture was centrifuged in a microfuge tube for 2 min at 8000 rpm. After resuspending in 50 µl of 1.2 M sorbitol, 50 µl of 0.1 mg/ml zymolyase T100 in 1.2 M

sorbitol was added. After incubating for 6-7 minutes at 30° C, 20 µl of the mixture was added to a YPD dissection plate and run down in a stripe. A dissection microscope with a fine-needle attachment was used to separate tetrads into spores (Figure 3.5).

2.5.4 Replica Plating

Dissected spores were grown on YPD and then patched onto fresh YPD plates. Using sterile velvet, the cells were transferred onto additional diagnostic plates in order to gather genotypic information with regard to resistance against Clonat and G418 (indicating presence of *NOT4* and *UBP3* gene deletion, respectively), as well as mating type.

2.6 Spot Plating of NOT4 RING Domain Mutants

2.6.1 Measuring Synthetic Lethality of NOT4/DEF1

NOT4/DEF1 double mutants surviving by the *URA3* wild type copy of *NOT4* (see section 2.4) were transformed with plasmids encoding mutations in Not4 functional domains: pRS415 (empty vector), pOP50 (wild type Not4-myc LEU2), pOP59 (Not4-myc 164A LEU2), and pOP61 (pNOT4-Myc6-Not4 (78-587)-LEU2). The same transformation protocol as in section 2.4 was followed, and the cells were plated on –LEU/-URA Dex plates.

Transformed cells were grown to saturation in –LEU2/Dex liquid media overnight at 30° C. The next day, dilutions in sterile water for each mutant were prepared to OD600 levels of 1.0, 0.1, and 0.01. 2 µl of each dilution was spotted onto 5-FOA media plates. The plates were incubated at 30° C, and images were taken at the 24, 48, 72, and 96 hour points.

2.6.2 Measuring Mutant UV-Sensitivity Phenotypes

BY4742 (wild type), JR1827 *not4*Δ, JR1828 *not4*Δ*rad26*Δ, and JR1824 *not4*Δ*ubp3*Δ cells were transformed with plasmids encoding mutations in Not4 functional domains: pRS415 (empty vector), pOP50 (wild type Not4-myc LEU2), pOP59 (Not4-myc 164A LEU2), and pOP61 (pNOT4-Myc6-Not4 (78-587)-LEU2). The same transformation protocol as in section 2.4 was followed, and the cells were plated on –LEU2/ Dex plates.

Transformed cells were grown to saturation in –LEU2/Dex liquid media overnight at 30° C. The next day, dilutions were for each mutant were prepared to OD600 levels of 1.0, 0.1, and 0.01 in sterile water. 2 µl of each dilution was spotted onto –LEU2 or –LEU2 + 50 mM hydroxyurea plates. Additional spotted –LEU2 plates were administered UV treatments of 30 J/m^2, 40 J/m^2, or 60 J/m^2 using a UV Stratalinker box (also see sections 2.7, 2.8). Plates were incubated in the dark at 30° C, and images were taken at the 24, 48, and 72 hour points.

2.7 Spot Plating to Qualitatively Assay Mutant DNA Damage Phenotypes

BY4742 (wild type), JR1698 *rad26*Δ, JR1700 *ubp3*Δ, JR1827 *not4*Δ, JR1828 *not4*Δ*rad26*Δ, and JR1824 *not4*Δ*ubp3*Δ yeast strains were grown overnight in liquid YPD media. The next day, dilutions for each strain were made to an OD600 of 1.0, 0.1, and 0.01 in sterile water, and 2.5 µl of each dilution for each strain was spotted onto plates designated for various treatments. The conditions tested were YPD control (30° C), YPD (37° C), YPD + 25 mM hydroxyurea (HU) (30° C), YPD + 50 mM HU (30° C), YPD + 75 mM HU (30° C), YPD + 20 J/M^2 (30° C), YPD + 40 J/M^2 (30° C), and YPD + 60 J/M^2 (30° C). To UV-treat cells, a UV

Stratalinker box was warmed-up for five minutes, and plates were then treated in the center of the unit. Cells treated with UV light were incubated in a dark cardboard box. Images were taken for each test at 24, 48, 72, and 96 hours.

2.8 UV Quantitative Assay of Mutant DNA Damage Phenotypes

BY4742 (wild type), JR1698 *rad26*Δ, JR1700 *ubp3*Δ, JR1827 *not4*Δ, JR1828 *not4*Δ*rad26*Δ, and JR1824 *not4*Δ*ubp3*Δ yeast strains were grown overnight to saturation in liquid YPD media. The next day, each strain was diluted to an OD600 of 1.0 in YPD. The following serial dilutions in YPD were prepared, according to the designated UV treatment: 3.3×10^4 and 10^4 for 0 UV; 3.3×10^4, 10^4, and 3.3×10^3 for 20 J/m^2; 3.3×10^4, 10^4, and 10^3 for 40 J/m^2; 3.3×10^3, 10^3, and 3.3×10^2 for 60 J/m^2. 0.15 mls of each dilution were plated in triplicate and treated with the specified amount of UV light. To UV-treat cells, a UV Stratalinker box was warmed-up for five minutes, and plates were then treated in the center of the unit. Cells treated with UV light were incubated in a dark cardboard box. After 48 hours (72 hours for slow-growing colonies), colonies were counted on each plate.

In order to generate a survival plot for each strain, the number of cells per treatment level was calculated by first averaging the triplicate number of colonies for each dilution factor. Then, the average value across dilution factors was obtained to represent the number of surviving cells at each treatment level. The number of cells present on plates without UV treatment was set to 100% survival, and number of cells at all other treatment levels was represented as a fraction of this total and plotted.

2.9 Measuring Rpb1 Degradation During 4-NQO Treatment

2.9.1 Growth and Treatment of Cells

BY4742 (wild type), JR1698 *rad26*Δ, JR1700 *ubp3*Δ, JR1827 *not4*Δ, JR1828 *not4*Δ*rad26*Δ, and JR1824 *not4*Δ*ubp3*Δ yeast strains were grown overnight to saturation in liquid YPD media. Strains were seeded in 75 ml of YPD in order to concurrently achieve an OD600 of 0.8 -0.9 in log phase growth the next day. 10 ml of cells were then removed as a 0 minute time-point. 15 mls of culture was removed and treated with 100 µg/ml cycloheximide (CHX) only for 120 minutes. The remaining cultures were treated with 6 µg/ml 4-Nitroquinoline 1-oxide (4-NQO) and 100 µg/ml CHX. 10 ml of this culture was removed at 30, 60, 90, and 120 minutes and processed to prepare whole cell extracts.

2.9.2 TCA Whole-Cell Extract Preparation

Cells were aggregated by centrifugation at 3.2 K in a J6 centrifuge for 5 minutes. Media was poured off, and 1 ml of cold 20% tricholoroacetic acid (TCA) was added to resuspend the cells. The suspension was transferred to a microfuge tube and centrifuged at 8k for 2 minutes. Supernatant liquid was removed by aspiration.

The cells were resuspended in 200 µl 20% TCA, and 250 µl glass beads were added and vortexed by hand twice for one minute. The tubes were transferred to a foam-head vortex mixer for 15 minutes at room temperature. After vortexing, the bottom of each tube was pierced with a sharp needle and placed within another microfuge tube. 400 µl of 5% TCA was added to the beads, and the dual-tubes were centrifuged briefly to allow the cells to collect in the bottom tube.

The new tubes were vortexed briefly and centrifuged in a microfuge at 6,000 rpm for 10 minutes at room temperature. Supernatant liquid was aspirated away, and 1 ml of 0.2 M Tris, pH 7.4 was added. The preparation was centrifuged for 5 minutes at 6,000 rpm, and wash solution was aspirated away. Tubes were placed on ice. 100 µl (or a volume adjusted to the OD600 of cells collected) of 0.2 M Tris, pH 7.4 was used to resuspend the pellet. 100 µl (or a volume adjusted to the OD600 of cells collected) of 3X SDS PAGE loading buffer was added, and cells were resuspended by vortexing. 1 µl of 1 M Tris, pH 8.0 was added to ensure the samples were not too acidic, and repeated until samples were blue in color. The tubes were boiled for five minutes, allowed to cool to room temperature, and mixed by vortexing. Sample were centrifuged at full speed for ten minutes, and the supernatant was transferred to a fresh tube and stored at -80° C. 5 µl of each sample was run on an SDS-PAGE gel for analysis.

2.9.3 Standardization of Protein Loading Amounts via Coomassie Gel

8% acrylamide 8 x 10 cm gels were poured, using 10 ml of running gel solution (prepared per 2 gels) and 10 ml of stacking gel solution (prepared per 4 gels). Running gel solution consisted of 2.5 ml 4X running gel buffer (1.5 M Tris-HCl, pH 8.8, and 0.4% SDS), 2.7 ml 30% acrylamide solution, 30 µl of 25% ammonium persulfate solution (APS) and 4.8 mls ddH2O. Stacking gel solution consisted of 2.5 ml stacking gel buffer (0.5 M Tris-HCl, pH 6.8 and 0.4% SDS), 1.3 ml acrylamide solution, and 6.3 ml ddH2O.

2 µl of TEMED was added to 1 ml of separating gel solution, and 0.5 ml of solution was added and allowed to polymerize in the gel apparatus as a “plug”. 10 µl of TEMED was added to the remaining gel solution, and a glass pipet was immediately used to pipet the remaining

solution down the side of the apparatus. The apparatus was filled until the separating gel was about 0.5 cm from the tips of the comb. 150 µl of water-saturated isobutanol was added down one side of the apparatus, and the separating gel was allowed to polymerize. After about ten minutes, butanol and unpolymerized material was poured off, and the gel was washed 3-4 X with ddH2O. The remaining drops of water were drained off.

50 µl of 25% APS and 15 µl of TEMED was added to the stacking gel solution. Immediately, the stacking gel solution was added above the separating gel using a glass pipet. The newly poured stacking gel was allowed to polymerize around the comb. Samples were boiled for 2-3 minutes prior to loading, and then run at 25-30 mA per gel in 1X Tris-Glycine SDS.

After the gel run, the stacking gel was removed and the separating gel was placed into 0.25% Coomassie blue R250 in 50% MeOH, 10% acetic acid. The gels were incubated with shaking for 30 minutes. The stain was removed, and gels were rinsed briefly with ddH2O. Gels were next incubated with Destain I solution (50% ethanol, 10% acetic acid) for 10 minutes, equal volumes of Destain I and Destain II (10% ethanol, 5% acetic acid) for 10 minutes, and Destain II overnight. Staining with Coomassie blue enabled visualization and standardization of protein loading amounts in anticipation of western blotting. Gels were stored in 5% acetic acid.

2.9.4 SDS-PAGE and Protein Transfer

Samples were run on SDS-PAGE gels as described in the previous section. After the gel run, proteins were transferred to nitrocellulose membranes using a semi-dry transfer procedure. 3-5 ml of transfer buffer (1X Tris-glycine-SDS, 20% methanol) was pipetted onto the surface of

the transfer apparatus. 3 pieces of Whatman paper (pre-soaked in transfer buffer) were layered on the apparatus one at a time. Air bubbles were removed by rolling a plastic pipet across the top of each paper. A "puddle" of transfer buffer was pipetted onto the stack, and the nitrocellulose membrane was layered on top. The gel was placed on the membrane, and air bubbles were again rolled out. Three additional pieces of Whatman paper were layered on the gel in a similar manner. Transfer buffer was pipetted over the lid of the transfer unit, and the lid was placed on the unit. A 1 kg weight was placed on the lid. Proteins were transferred at 80-90 mA per gel for 45 minutes.

The membranes were removed from the transfer unit and placed in Ponceau S stain (2% acetic acid and 0.2 % Ponceau S) for 3-5 minutes. The stain was partially removed by rinsing with ddH2O, marker positions were noted in pencil, and the membranes were completely destained in TBST (50 mM Tris HCl, pH 7.4, 150 mM NaCl, 0.1% Tween 20).

2.9.5 Western Blotting and Protein Detection Via ECL

Nitrocellulose membranes were rinsed in ddH2O and trimmed at the 100 kDa mark; above this, membranes were probed for Rpb1 (8WG16 1:1000, mouse), and below, membranes were probed for Taf68 housekeeping protein (Taf68 R1 BO, 1:1000). The membranes were placed in blocking solution (5% BSA in TBST) for 1 hour with shaking at room temperature. After blocking, membranes were placed in in primary antibody incubation solution (1% BSA) overnight with gentle rolling at 4° C. The membranes were washed twice for 5 min. in incubation solution at room temperature and then incubated in a 1:5000 dilution of secondary antibody for 60 minutes (donkey anti-mouse HRP from Amersham for Rpb1 probing; donkey

anti-rabbit HRP from Amersham for Taf68 probing). After incubation, the membranes were washed once for 5 minutes and once for 10 minutes in incubation solution, and then washed twice for 5 minutes in TBST before detection by ECL.

Blots were placed in 5 ml of ECL Reagent A mixed with 5 ml of ECL Reagent B (Amersham) and allowed to incubate for about 1 minute with gentle shaking. The blots were placed on a glass plate and covered with plastic wrap, and then exposed in the dark to x-ray film for 20 seconds-3 minutes.

2.9.6 Generating Rpb1 Degradation Plots

ECL films were scanned using a flat-top scanner, and the gel images were quantified using NIH ImageJ software. Images were converted to 16-bit grayscale format. A rectangular region of interest (ROI) was defined to surround the largest band present in a given gel, and the mean gray value was taken for each band using the fixed ROI. This was the "density value" used to construct a plot of Rpb1 degradation. Plotted points were generated by obtaining the density value for each band, and dividing each Rpb1 density value by the corresponding Taf68 control density value. The value for the 0-minute time-point was set to 100%, and each subsequent time-point was calculated as (Value for time-point X)/(Value for time-point 0) x 100 in order to achieve values measured as a percentage of initial Rpb1 levels.

Chapter 3

Results

3.1 Selection and Verification of Yeast Mutants

In order to study the genetic interactions of Ccr4-Not with proteins in the TCR and ubiquitin/proteasome pathways, yeast mutants with single *NOT4, UBP3, RAD26,* and *DEF1* deletions were obtained alongside mutants with double *NOT4/UBP3* and *NOT4/RAD26* deletions.

RNAPII Degradation Factor, or Def1, has been shown to enable the ubiquitylation and eventual proteolysis of RNAPII that has been stalled by a DNA lesion. Def1 binds in a complex with Rad26 in chromatin, but does not function in TCR. Instead, Def1 mediates a "last resort" response to lesion-stalled RNAPII, facilitating degradation when rapid Rad26-promoted DNA repair is not possible. (60) Thus, the cell retains multiple pathways to contend with DNA damage-induced interruptions to transcription. The known impact of decreased RNAPII degradation in *not4*Δ cells under DNA-damaging conditions (30) prompted an investigation into the combined phenotypic effect of *NOT4/DEF1* double deletion in yeast.

Rad26 and Ubp3 act in complementary ways to regulate the cellular response to DNA damage and consequent transcriptional arrest. While Rad26 is involved in transcription-coupled nucleotide excision repair, permitting the cell to remove UV-induced DNA lesions, Ubp3 is a ubiquitin protease which removes ubiquitin from stalled RNAPII. Ubp3 thereby functions as a means of stalling "last resort" RNAPII degradation in response to transcriptional arrest, allowing additional time for the cell to first repair the damage and resume transcription before degrading RNAPII (see sections 1.3, 1.4). Understanding the relationship of these proteins with Not4, an

E3 ubiquitin ligase whose deletion impacts levels of RNAPII degradation under stress, provides critical information regarding how multiple DNA-damage response pathways may operate within the cell.

Generation of single mutants proceeded through the application of PCR-generated knockout cassettes, using a method described by Brachmann, et al (Figure 3.1). In this method, we used versions of the pRS40X plasmid, containing different selectable markers, to produce a PCR fragment of interest which was amplified and then purified with ethanol precipitation (section 2.2 and 2.3.2). This fragment is termed a PCR knockout cassette, which is then used to replace a gene of interest in yeast after transformation. Yeast containing the deletion are plated on selective media based on the marker used, so that isolation of mutants can occur via complementation. Because not all clones designated positive for the marker gene are actual mutants—recombination can occur between genomic DNA and the transformed PCR product—mutants must also be verified by PCR (Figure 3.1). One set of primers, termed ORF diagnostic primers, prime within the open reading frame of the gene to be deleted and thus will produce no PCR product. In tandem, a gene-specific diagnostic primer is used to prime upstream of the integration site while a downstream marker-specific diagnostic primer primes downstream on the marker sequence. This set of primers will produce a PCR product when the gene has been replaced by the marker.

This strategy was employed to delete the *DEF1* gene in already existing *not4*Δ mutants containing a *URA3*-marked *NOT4*-HA tagged wild type plasmid. Straightforward knockout of *DEF1* in the *not4*Δ mutant was not possible via successive transformation of PCR-generated gene knockout cassettes or mating and dissection, as neither approach produced viable double mutants (see the following section). A *DEF1::HIS3* cassette was produced using the pRS403

plasmid and detected on an agarose gel (Figure 3.2, A). The *not4*Δ cells were then transformed with this knockout cassette and plated onto –HIS/-URA media in order to select for both the plasmid and the newly introduced cassette. *def1*Δ mutants are known to grow slowly, so only small colonies were selected. Mutants were then verified via an ORF diagnostic primer test (Figure 3.3, A).

Generation of the *not4*Δ*rad26*Δ double mutant proceeded in a similar manner. Genomic DNA was prepared from an already existing Clonat resistant *not4*Δ*::NATMX* strain and used as a template to generate a *NOT4* knockout cassette. The cassette was first detected on an agarose gel and subsequently gel purified (Figure 3.2, B, C). Cells with an already existing *rad26*Δ::*KANMX* (G418 resistant) background were transformed with the newly produced cassette and grown on YPD media containing Clonat. Because *NOT4* deletion mutants are already known to be slow-growing, only small colonies were selected for further testing. The *not4*Δ*rad26*Δ double mutants were verified using both ORF diagnostic primers and gene-specific/marker-specific primers (Figure 3.3, B).

The *NOT4/UBP3* double deletion mutant was produced via yeast mating and dissection. This strategy takes advantage of the yeast life cycle, which includes both haploid and diploid phases. Haploid yeast have two mating types—MAT a and MAT α. When cells of distinct mating types are brought together, they will mate via a cell fusion event and form diploid yeast which reproduce normally by mitosis. However, nutritional starvation will induce the sporulation of diploids, in which four haploid meiotic progeny are formed (Figures 3.4, 3.5). Meiosis leads to the segregation of mutant alleles in which a gene of interest has been deleted: one spore will be a “double mutant”, containing both deletions, two spores will be “single mutants”, and one spore will contain no deletions. Replica plating of the spores onto selective

media allows the new haploids to be "scored" for various markers and mating type, thereby permitting the identification of new double yeast mutants.

The *not4*Δ*ubp3*Δ strain was generated by mating *not4*Δ::*NATMX* single mutants (of MAT α mating type) with *ubp3*Δ::*KANMX* single mutants (of MAT a mating type) and screening for diploids on media containing both Clonat and G418 antibiotic. Because *not4*Δ mutants grow slowly, subsequent sporulation and dissection of the diploids yielded tetrads that contained two slow-growing spores and two fast-growing spores. The dissected tetrads were patched onto YPD and replica plated in order to look for spores that were capable of growing on both Clonat and G418 media (suspected double mutants). These potential mutants were then screened and verified by a PCR diagnostic test (Figure 3.3, C).

3.2 Simultaneous *NOT4/DEF1* Deletion is Lethal in Yeast

"Straightforward" attempts to achieve a double *not4*Δ*def1*Δ yeast mutant, such as by mating and dissection or successive transformation of PCR-generated gene knockout cassettes, proved to be ineffective. These multiple failed attempts suggested that *def1*Δ and *not4*Δ may be synthetically lethal in combination. Synthetic lethality suggests the presence of a redundant pathway or direct protein interaction—while parent single mutants are viable, the combined knockout of two synthetically lethal genes exacerbates the cell phenotype to the point of death (12).

To investigate this possibility, *not4*Δ mutants were transformed with a *URA3*-marked plasmid containing a wild type copy of *NOT4* (pRS416-NOT4-HA), and subsequently

transformed with the *DEF1::HIS3* knockout cassette. This strategy yielded a *not4*Δ*def1*Δ genomic double mutant that (importantly) retained Not4 functionality via the wild type plasmid. Plating these mutants on media containing 5-Fluorootic Acid (5-FOA), however, resulted in a total loss of growth. The *URA3* gene encodes orotidine 5'-phosphate decarboxylase (OMP decarboxylase), which catalyzes the decarboxylation of 5-FOA to 5-fluorouracil, a toxic compound. Therefore, only cells capable of dispensing the *URA3* plasmid will survive in the presence of 5-FOA (3). The inability of the *not4*Δ*def1*Δ double mutants to grow on 5-FOA media thus indicates a synthetically lethal interaction between *DEF1* and *NOT4*, as the cells were not able to survive without *NOT4* present.

To verify and measure the synthetic lethality of the *not4*Δ*def1*Δ strain, and to test the requirement of the Not4 RING domain, double mutant cells surviving by the *URA3* wild type copy of *NOT4* were transformed with wild type and mutant version of *NOT4* on a *LEU2*-marked plasmid. The Not4 I64A point mutant plasmid, pOP59, (in which isoleucine is replaced with alanine at position 64) interrupts the interactions of Not4 with its E2 ubiquitin-conjugating enzymes, Ubc4 and Ubc5 (37, 39). Another mutant plasmid, pOP61, eliminates the Not4 RING domain entirely. The cells were grown overnight in –LEU/Dextrose liquid media, which, containing uracil, allows a fraction of cells to excise the *URA3* plasmid if it is possible to survive without it. Growth of the transformed cells was then tested via a spot-assay on 5-FOA media, at time-points of 24, 48, and 72 hours (Figure 3.6).

Only double mutants that were transformed with the *LEU2*-marked wild type copy of *NOT4* displayed growth after 72 hours, verifying the existence of a synthetically lethal interaction between *NOT4* and *DEF1* (Figure 3.6). Additionally, the assay indicates that the Not4 RING domain is required to contend with the lethal effects of simultaneous *NOT4/DEF1*

deletion, as mutants which included a RING domain disruption or deletion were not viable. The RING domain is responsible for the ubiquitylation activity of Not4, and its deletion has been shown to impact the degradation of RNAPII *in vivo* during stress conditions (30). Its requirement in the synthetic lethality of *NOT4/DEF1* corroborates this result, and suggests that a pathway redundancy between *NOT4* and *DEF1* may be related to the role of these proteins in enabling the degradation of RNAPII. Shown also is the growth of single mutants transformed with an empty vector or the wild type *NOT4* plasmid, whose growth is robust when compared with double mutants. These cells do not need to contend with the residual lethal effects of *URA3* plasmid interaction with 5-FOA.

3.3 *NOT4/UBP3* Double Mutants Show Greater Resistance to DNA Damage than *NOT4* Single Mutants

Unlike *not4*Δ*def1*Δ double mutants, deleting *NOT4* in combination with *RAD26* or *UBP3* resulted in cells that were viable. Therefore, we investigated how deletions in these genes elicited other phenotypes in yeast, especially during DNA-damaging or otherwise stressful conditions. The growth of *rad26*Δ*, ubp3*Δ*,* and *not4*Δ single deletion mutants, along with *not4*Δ*rad26*Δ and *not4*Δ*ubp3*Δ double deletion mutants, was tested via a spot assay. Each mutant was assayed under a variety of stress conditions: at higher-than-normal growth temperature (37° C), in the presence of hydroxyurea, and in the presence of UV light. Hydroxyurea (HU), an inhibitor of ribonucleotide reductase, inhibits DNA replication in yeast by starving the cell for dNTPs (26). The drug was combined with YPD at concentrations of 50 mM and 75 mM. UV light was applied at levels of 20 J/m^2, 40 J/m^2, and 60 J/m^2.

Under normal growth conditions (YPD at 30° C), *rad26*Δ and *ubp3*Δ single mutants grew robustly, at a rate that was very similar to wild type yeast. In contrast, *not4*Δ single and double mutants show reduced growth, although *not4*Δ*rad26*Δ mutants seemed to grow at a level that was slightly higher than *not4*Δ or *not4*Δ*ubp3*Δ mutants (Figure 3.7). In the presence of HU, however, notable differences between separate *not4*Δ mutants emerge: wild type, *rad26*Δ, and *ubp3*Δ show strong growth compared to weakly growing *not4*Δ and *not4*Δ*rad26*Δ mutants, but *not4*Δ*ubp3*Δ mutants grow more robustly than the other *not4*Δ mutant varieties.

In the presence of DNA-damage inducing UV light, these qualitative differences in growth were both recapitulated and made visible in finer resolution. At a low level of UV radiation (20 J/m^2), wild type, *rad26*Δ, and *ubp3*Δ cells grow robustly compared to all three *not4*Δ mutants. When UV radiation is increased (40 J/m^2), wild type, *rad26*Δ, and *ubp3*Δ cells continue to show strong growth (at high levels of radiation, however, all strains exhibit an abnormal growth phenotype characterized by asymmetrical colony formation). But among *not4*Δ mutants, levels of *not4*Δ*ubp3*Δ growth appear to surpass those of *not4*Δ and *not4*Δ*rad26*Δ cells. Simultaneous deletion of *UBP3* thus suppressed the DNA damage sensitivity of the *not4*Δ mutant.

When placed at 37° C, *not4*Δ single and double mutants show a lack of growth compared to wild type, *rad26*Δ and *ubp3*Δ yeast (Figure 3.8). Increased growth temperature affects translation of proteins, leading to stalled ribosomes with translationally arrested products. Temperature sensitivity of *not4*Δ mutants has been characterized previously and is related to the role of Not4 in clearing nascent protein chains after translational arrest.(15) Because simultaneous deletion of *UBP3* results in double mutants that are still temperature sensitive,

*ubp3*Δ suppression of damage sensitivity seems to be specific to DNA damage responses, rather than broadly suppressing stress response defects.

While the spot assay provides a crude overview of possible differences among the mutants in response to stress conditions, it does not provide the sensitivity required to quantify subtle phenotypes. To examine these phenotypes in greater detail, a quantitative test of mutant UV-sensitivity was employed. In this test, the yeast mutants were grown overnight in liquid YPD media until saturation. The cultures were then diluted to a uniform density in YPD, plated in serial dilutions, and then treated with UV light (see section 2.8). After 48 hours (72 hours for slow-growing colonies), the resulting colonies were counted. Cell growth under UV treatment was calculated as a fraction of control growth (colonies formed on YPD without any UV treatment). The experiment was performed using triplicate YPD plates for each dilution and corresponding UV treatment (error bars in Figure 3.9 show standard deviation among counted plates), and the findings were reproduced in a second, independent test (not shown).

In wild type yeast, roughly 75% of cells remain after 20 J/m^2 of UV treatment, which decreases to about 20% after 40 J/m^2, and 10% after 60 J/m^2 (Figure 3.9). *ubp3*Δ yeast were the only mutants with a higher survival rate, retaining about 25% of cells after treatment with 60 J/m^2 of UV radiation. This agrees with previously reported findings that *ubp3*Δ yeast are less sensitive to UV radiation (28). In contrast, *rad26*Δ yeast displayed more UV sensitivity than the wild type, retaining about 3% of cells after treatment with 60 J/m^2 of UV radiation. Among the *not4*Δ mutants, about 1.5% of single mutant *not4*Δ yeast survived after treatment with 60 J/m^2 of UV radiation, while, in comparison, about 0.5% and 2% of *not4*Δ*rad26*Δ and *not4*Δ*ubp3*Δ cells survived, respectively. The decreased UV-sensitivity of the *not4*Δ*ubp3*Δ strain corroborates the trends observed in spot assays. Additionally, this finding complements the observations of Kvint

et al., who reported that *UBP3* deletion promotes UV survival in mutant cells that were already repair-compromised (28). The results suggest that deletion of *UBP3* (normally responsible for deubiquitylating stalled RNAPII) promotes increased RNAPII degradation in response to DNA damage, thereby offering a protective effect on UV survival.

Finally, a spot-assay was performed to assess the role of Not4 functional domains in mutant stress response (Figure 3.10). Wild type, *not4*Δ, *not4*Δ*ubp3*Δ, and *not4*Δ*rad26*Δ cells were transformed with wild type and modified versions of *NOT4* on a *LEU2*-marked plasmid. The plasmids used were the same as in the test for *not4*Δ*def*Δ synthetic lethality (section 3.2). The Not4 I64A point mutant plasmid, pOP59, (in which isoleucine is replaced with alanine at position 64) interrupts the interactions of Not4 with its E2 ubiquitin-conjugating enzymes, Ubc4 and Ubc5 (37, 39). The pOP61 plasmid eliminates the Not4 RING domain entirely. The cells were plated on HU-containing media, and growth was assessed at 24, 48, and 72 hours. Each mutant strain transformed with either an empty vector (pRS415) or the mutant Not4 RINGΔ plasmid showed impaired growth, indicating that the RING domain is required to resolve the stress phenotype. Growth was restored in mutants transformed with the wild type Not4 plasmid or the I64A point mutant plasmid, in which whole or partial RING domain activity was restored.

3.4 Rpb1 Degradation in Response to DNA Damage in *NOT4* Double Mutants

After testing their growth phenotypes under stress, we next sought to understand how each mutant degrades RNAPII in response to DNA damage. RNAPII degradation occurs via the polyubiquitylation of Rpb1, its large subunit. The E3 ligase Rsp5 binds the subunit by its CTD,

and adds mono-ubiquitin to the main body of Rpb1 (18; also see section 1.4). After sensing mono-ubiquitin, Elc1/Cul3 (Elongin Cullin) polyubiquitylates Rpb1 to promote degradation. This degradation pathway may only be active when RNAPII is stalled by DNA damage, and is perhaps initiated as a consequence of Def1/Rad26 interaction (60). However, the Rbp1 degradation in response to DNA damage only occurs as a "last resort," mediated by the action of the Ubp3 ubiquitin protease. It has already been shown that UV-irradiated yeast lacking *UBP3* have higher *in vivo* levels of ubiquitylated RNAPII which is rapidly degraded, thereby affording these cells less sensitivity to DNA damage (28). Given the lack of Rbp1 degradation observed in *not4*Δ mutants (20), observing the combined phenotypic effect on Rpb1 degradation in both *not4*Δ*ubp3*Δ and *not4*Δ*rad26*Δ mutants can yield insight into how multiple DNA damage repair pathways may operate in eukaryotes.

In order to measure Rbp1 degradation in the various mutants, cells were grown in media containing 4-Nitroquinoline 1-oxide (4-NQO) over a two-hour time-course. Growing yeast in the presence of 4-NQO mimics the biological effect of DNA-damaging UV light, producing excisable 4-NQO-purine adducts that can be repaired via TCR (21). Cycloheximide was also included in the growth media to prevent new protein synthesis, so the overall degradation of RNAPII could be assayed without the presence of newly synthesized Rpb1. Experimental time-points were taken every thirty minutes, and the amount of Rpb1 was quantified at each time-point. In order to normalize the amount of Rpb1 present in each sample, measurements of Taf68, a housekeeping protein, were also taken.

Accurate quantification of Rpb1 levels was not possible at every time point, and was likely due in part to slight differences in protein loading that could not be resolved by normalization with a loading control. There were additional problems with antibody detection

by ECL (for example, the 60 minute time-point of the *not4*Δ single mutant assay displays a broken band). Notably, the Taf68 control measurements were taken using a nonspecific, cross-reacting band, as the Taf68-specific band was over-exposed. However, Figure 3.11 allows for an assessment of general trends in Rpb1 destruction during DNA damage among the various mutants.

In wild type cells, Rpb1 levels decreased to about 30% of initial levels after 120 minutes of treatment with 4-NQO. Rpb1 was more quickly degraded in *ubp3*Δ mutants, displaying sharply lower levels (an approximate tenfold reduction) after only thirty minutes in contact with 4-NQO (Figure 3.11). After 120 minutes, Rpb1 levels in *ubp3*Δ cells was reduced to roughly 5% of the initial level. This is in agreement with published work (28). In *rad26*Δ cells, Rpb1 turnover is also higher than in the wild type, though not to the same extent as *ubp3*Δ. After 120 minutes, Rpb1 levels were reduced to roughly 20% of initial levels. Accelerated Rpb1 degradation in *rad26*Δ mutants also reflects previously published findings, and suggests a role for Rad26 in preventing premature degradation of RNAPII by Def1 (60).

In *not4*Δ mutants, Rpb1 turnover in response to 4-NQO was reduced, as predicted. Rpb1 levels were reduced to about 60 – 80% of the initial value, in agreement with previous laboratory findings (30). Among *not4*Δ*ubp3*Δ mutants, difficulties in quantification resulted in an apparent strong increase in Rpb1 levels after 30-60 minutes of 4-NQO exposure that was not reflective of actual biological phenomenon. This was probably due to variations in protein level from TCA preparation, as well as improper normalization by the Taf68 cross-reacting band. After 120 minutes, however, Rpb1 levels in the *not4*Δ*ubp3*Δ strain were reduced to about 40 – 50% of the initial value, indicating accelerated degradation compared to *not4*Δ mutants. In *not4*Δ*rad26*Δ mutants, Rpb1 appeared to be degraded even more, retaining only about 10 – 20% of original

Rpb1 levels. These results indicate that Not4 is not strictly necessary for RNAPII decay after DNA damage. Removing other blocks to degradation in conjunction with a *NOT4* deletion (such as deubiquitylation of RNAPII by Ubp3, or inhibition of Def1 by Rad26) appear to permit Rpb1 turnover through other means.

Figure 3.1: Schematic of PCR-Mediated Gene Knockout in Yeast

A.

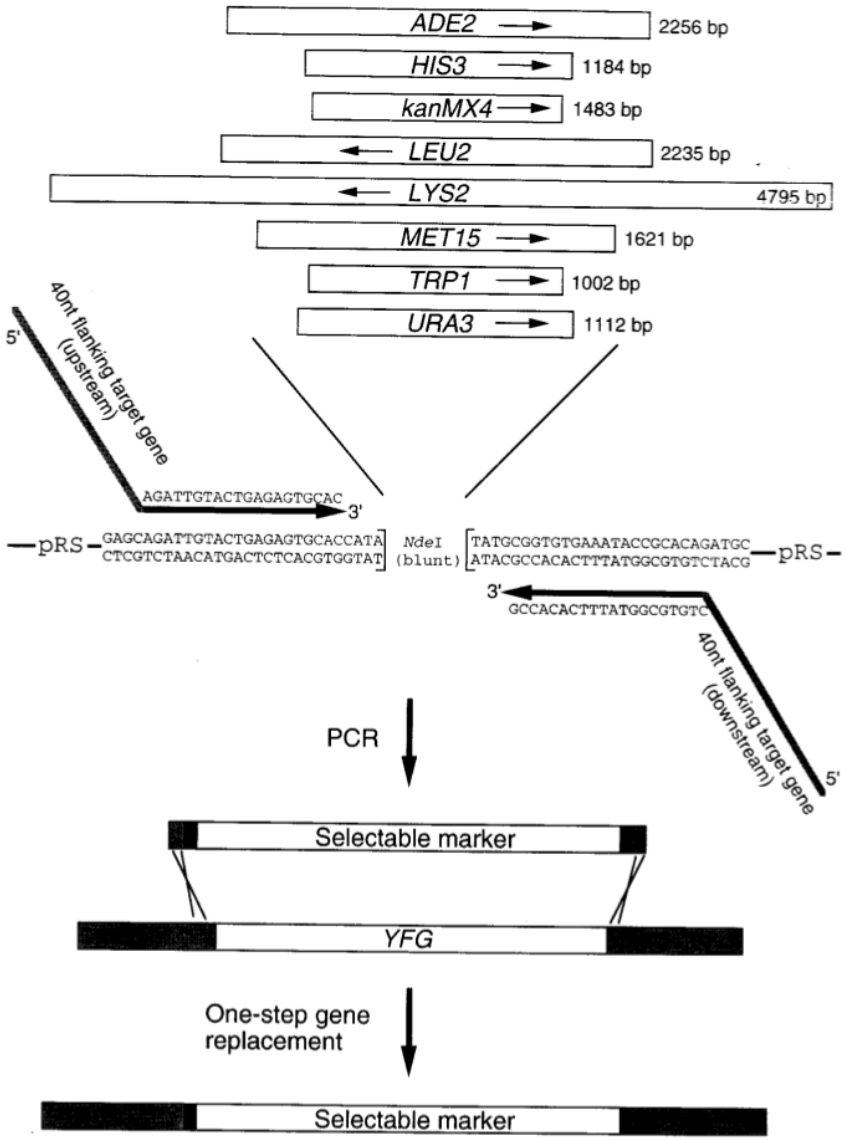

B.

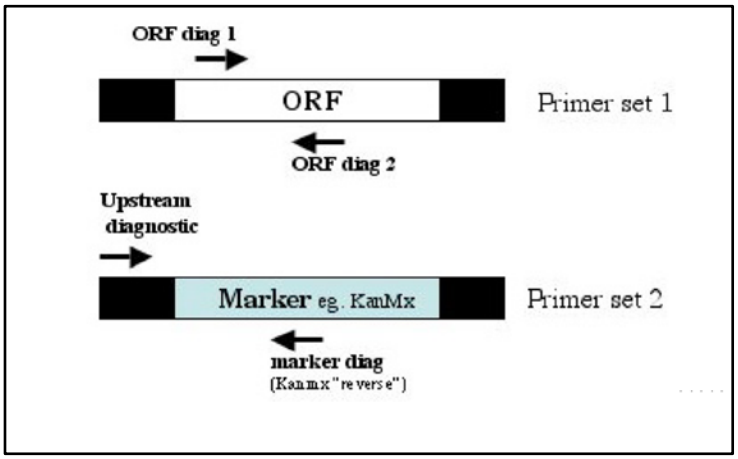

Figure 3.1: Schematic of PCR-Mediated Gene Knockout in Yeast. Taken from (5) (A), Reese lab protocol (B). (A) Various selectable markers have been inserted into the pRS40X series of plasmids, which may then be amplified to contain 40 nucleotide flanking sequences on either side of the marker, specific to a gene of interest. The flanked markers are PCR knockout cassettes, which may then be transformed into yeast. This strategy takes advantage of the fact that linear fragments of DNA can effectively mediate homologous recombination in yeast (Brachmann). (B) This diagram illustrates the process of verifying mutants by PCR. Because ORF diagnostic primers bind within the sequence that has been deleted, no PCR product should be formed. In contrast, a gene-specific upstream primer combined with a marker-specific downstream primer will produce a PCR product.

Figure 3.2: Generation of PCR Knockout Cassettes

A.

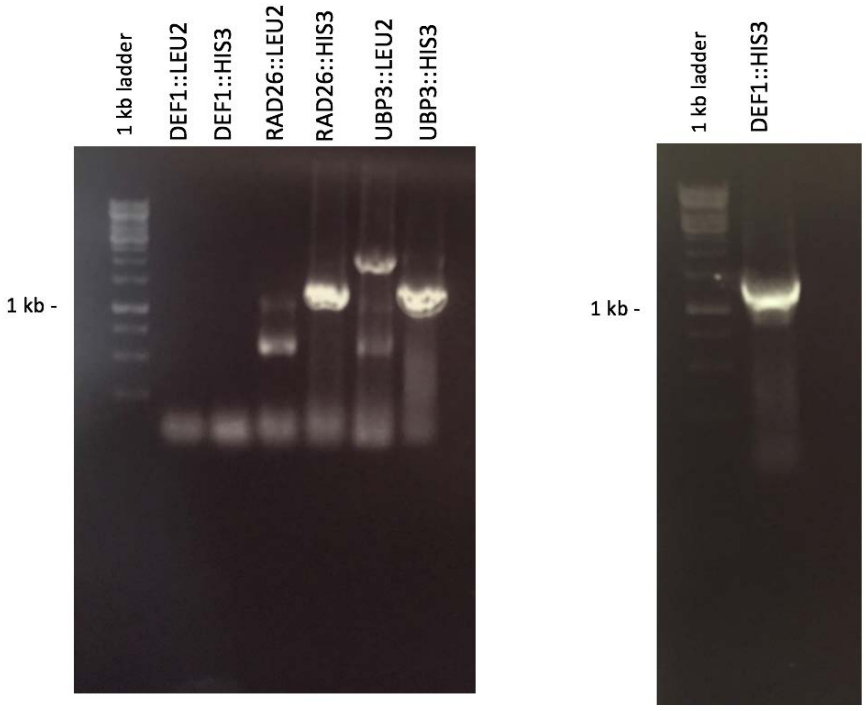

B.

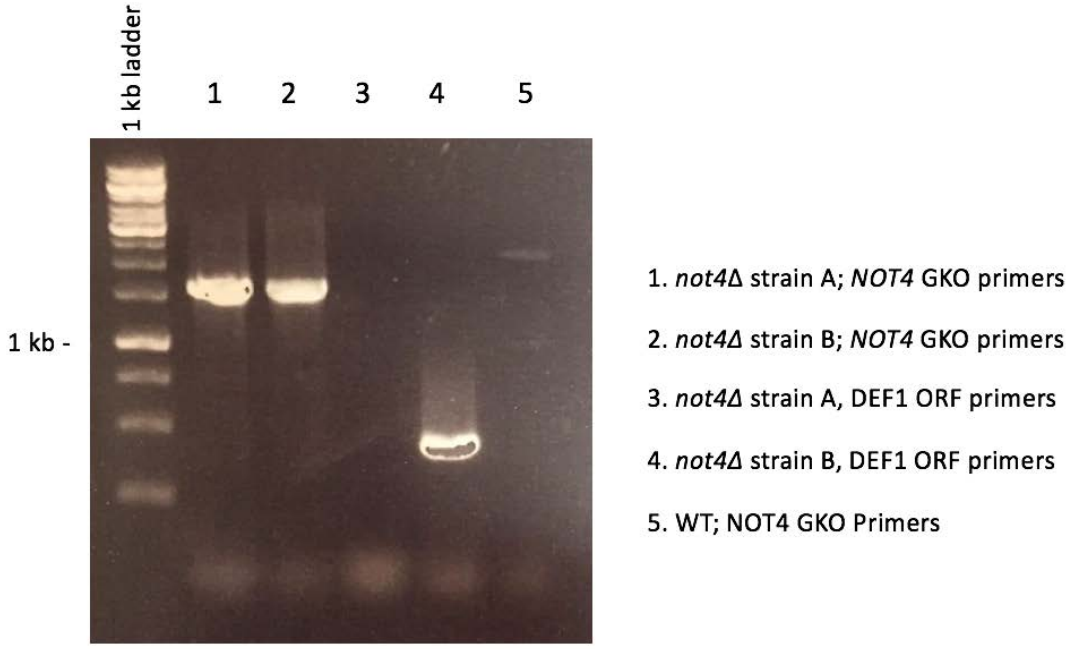

C.

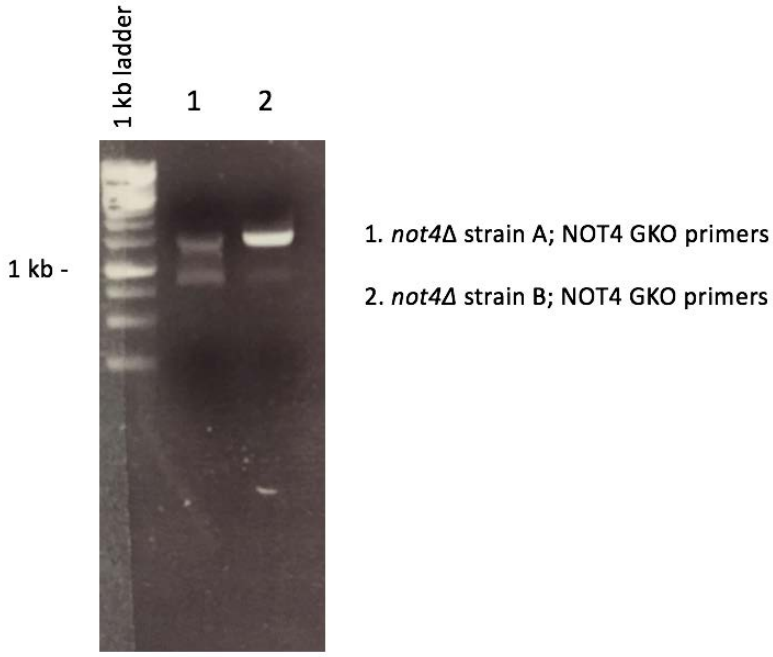

Figure 3.2: Generation of PCR Knockout Cassettes. (A) Generation of the *DEFI::HIS3* cassette. In the first gel, generation of the *DEF1::HIS3* cassette was not successful, apparently due to a failed PCR reaction. New primers were used to successfully generate the cassette, as seen in the second gel. (B) Generation of the *NOT4::NATMX* cassette using genomic DNA from a *not4*Δ mutant. The first two lanes show generation of the knockout cassette, while the remaining lanes serve as controls to ensure that both the PCR reaction is working correctly (*DEF1* primer lanes) and correct PCR product has been formed (checked by using *NOT4* gene knockout primers on the wild type strain). (C) *NOT4::NATMX* knockout cassette post gel-purification. The knockout cassette produced using the "B" strain was used for the remainder of the experiment.

Figure 3.3: Primer Tests For Mutant Verification

A.

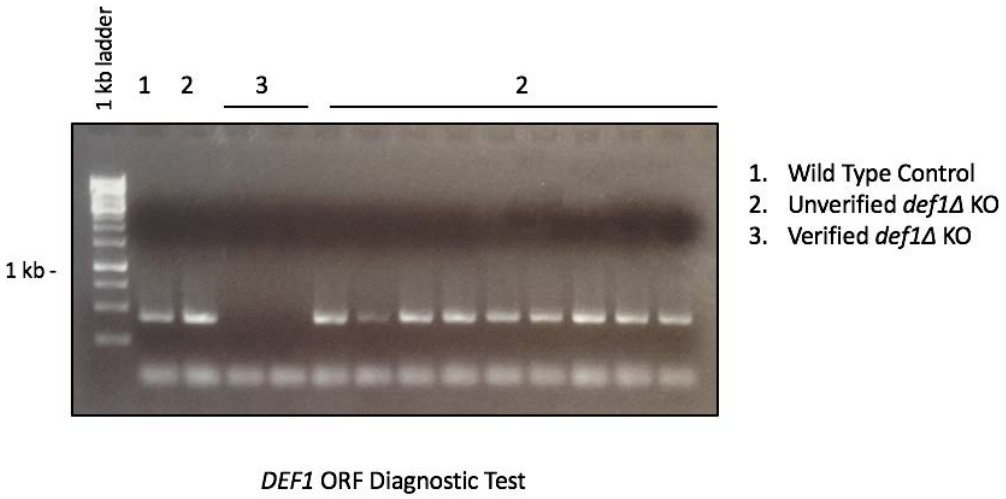

DEF1 ORF Diagnostic Test

B.

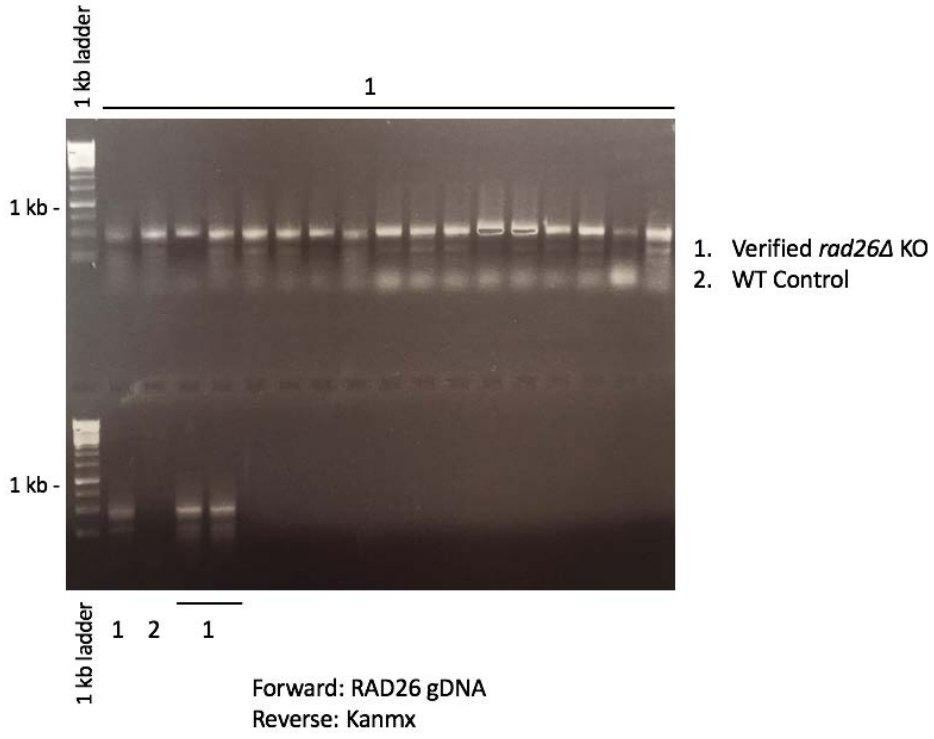

C.

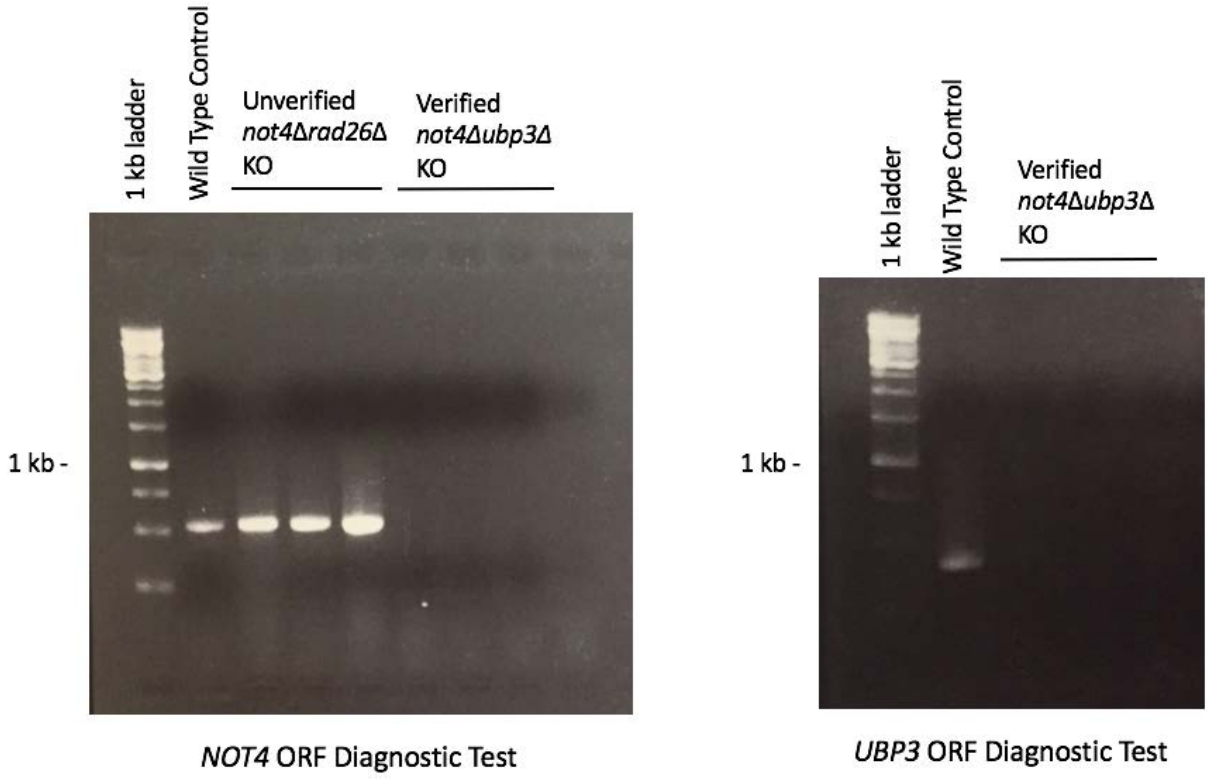

Figure 3.3: Primer Tests for Mutant Verification. Genomic DNA was isolated from suspected mutants growing on selective media, after transformation with a PCR knockout cassette. (A) ORF diagnostic primers show a gene deletion of *DEF1* has occurred in lanes missing any PCR product. (B) In contrast, gene-specific and marker-specific primer tests will produce a PCR product when the knockout is successful, indicating that *RAD26* is deleted. (Note that there is no PCR product in the wild-type control). (C) ORF diagnostic test confirms both a *NOT4* and *UBP3* deletion.

Figure 3.4: The Budding Yeast Life Cycle

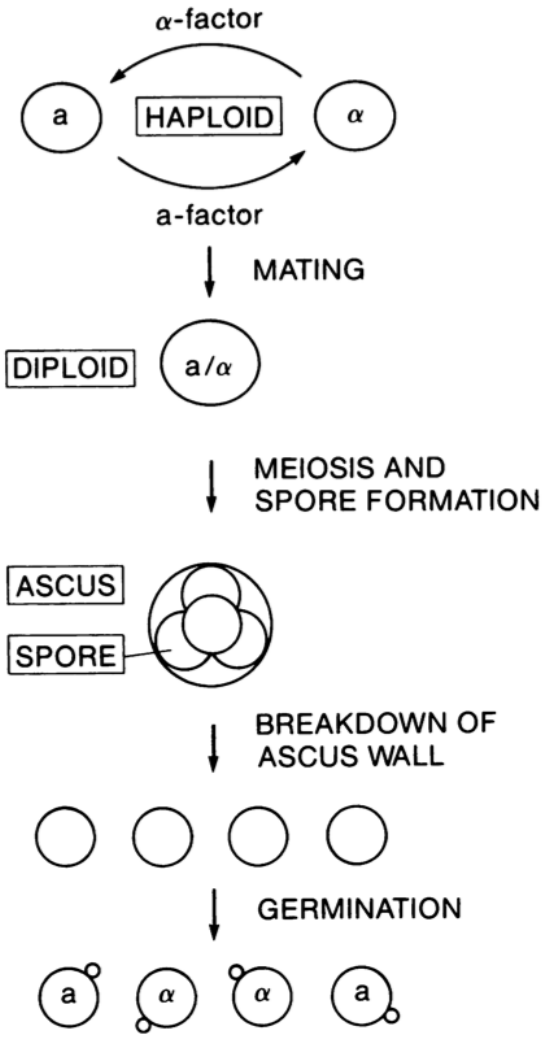

Figure 3.4: The Budding Yeast Life Cycle. Taken from (20). MAT a, MAT α, and MAT a/α (diploid) cells are all capable of reproducing normally by mitosis. However, when MAT a and MAT α cells mate to form a diploid cell, subsequent nutrient starvation will induce meiosis and sporulation. Within the tetrahedral ascus, four spores are formed: half are MAT a, and half are MAT α.

Figure 3.5: Tetrad Dissection Plate

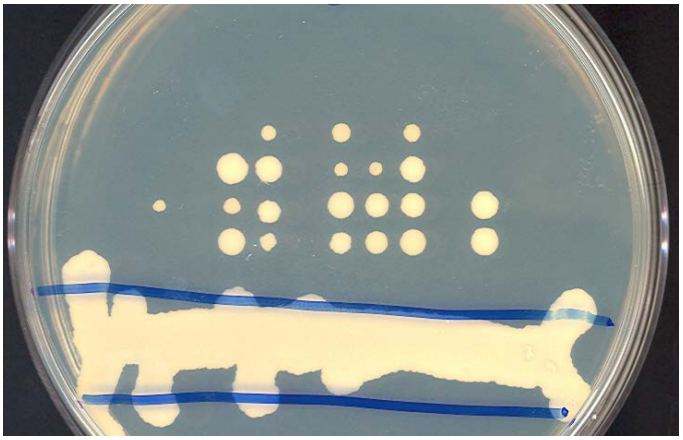

Figure 3.5: Tetrad Dissection Plate. This is an example dissection, produced via the mating and sporulation of *rad26*Δ and *ccr4*Δ haploid cells. Yeast tetrads are selected from the "dissection stripe" (shown at the bottom of the image) and separated into individual spores, aligned vertically. "True" tetrads will contain two slow-growing colonies (attributed to the slow growth of *ccr4*Δ mutants) and two fast-growing colonies, in which *CCR4* is not deleted.

Figure 3.6: Simultaneous *NOT4/DEF1* Deletion is Lethal in Yeast

A.

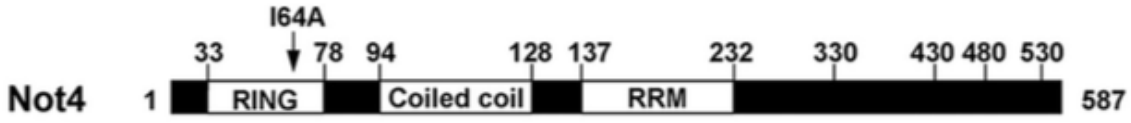

B.

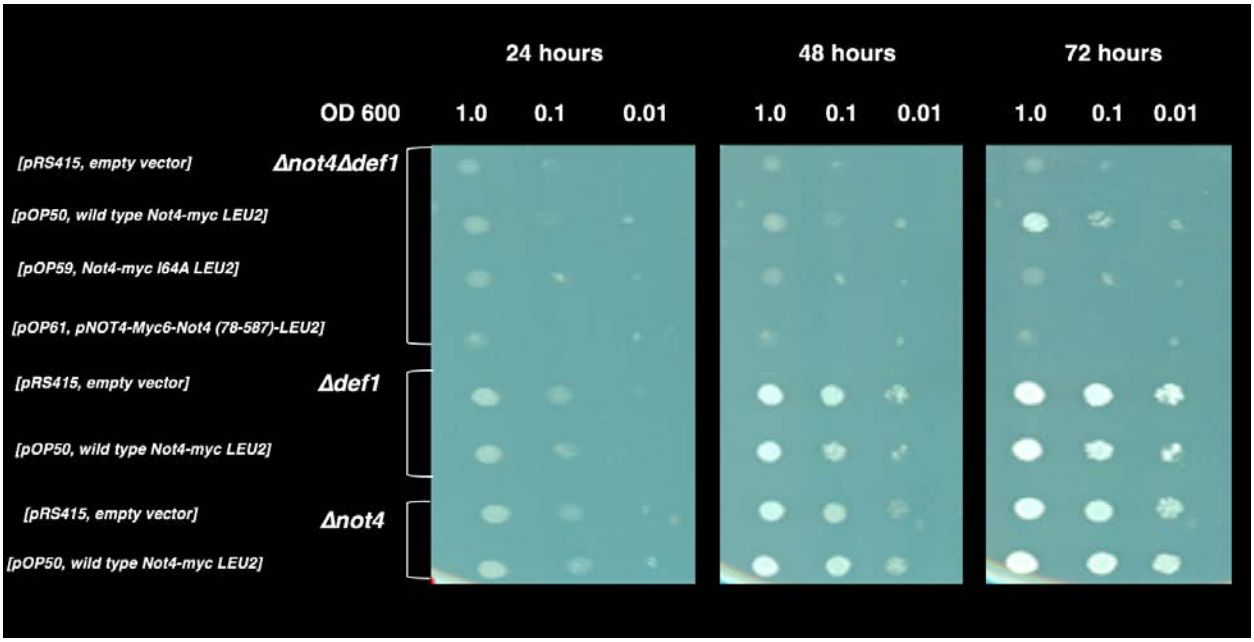

Figure 3.6: Simultaneous *NOT4/DEF1* Deletion is Lethal in Yeast. A "plasmid shuffle" experiment was performed in which yeast *not4*Δ*def1*Δ double mutants (surviving by a wild type copy of *NOT4* on a *URA3*-marked plasmid) were transformed with wild type and modified versions of *NOT4* on a *LEU2*-marked plasmid. (A) Taken from (38). This schematic of the Not4 protein indicates the positions of its functional domains: RING, coiled-coil (putative), and RNA-recognition motif (RRM). The pOP59 plasmid includes an I64A point mutation, interrupting the interactions of Not4 with its E2 ubiquitin-conjugating enzymes. The pOP61 plasmid entirely eliminates RING domain function. (B) Cells were grown overnight in –LEU/Dextrose media, which allows a portion of cells to lose the *URA3* plasmid if it is still possible to survive without it. Subsequent plating on 5-FOA media induces a lethal response in cells which cannot discard the *URA3* plasmid, thereby selecting for cells that can survive without the wild type copy of *NOT4*. Shown also is the growth of single mutants transformed with an empty vector or the wild type *NOT4* plasmid.

Figure 3.7: Mutant Phenotype Response to DNA-Damaging Conditions

A.

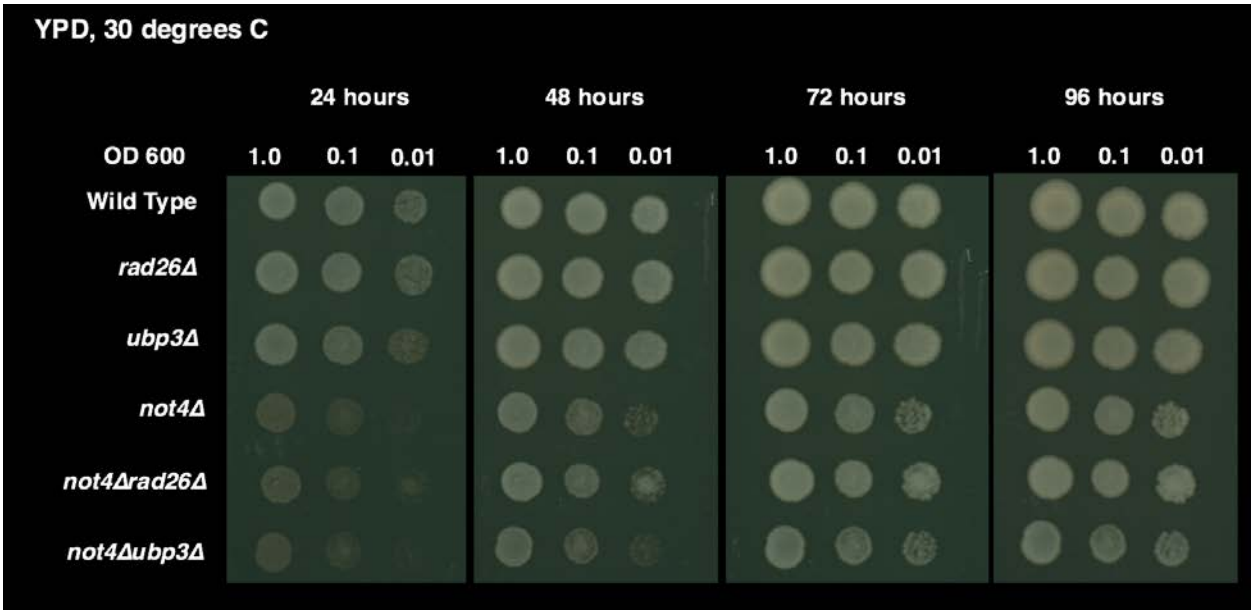

B.

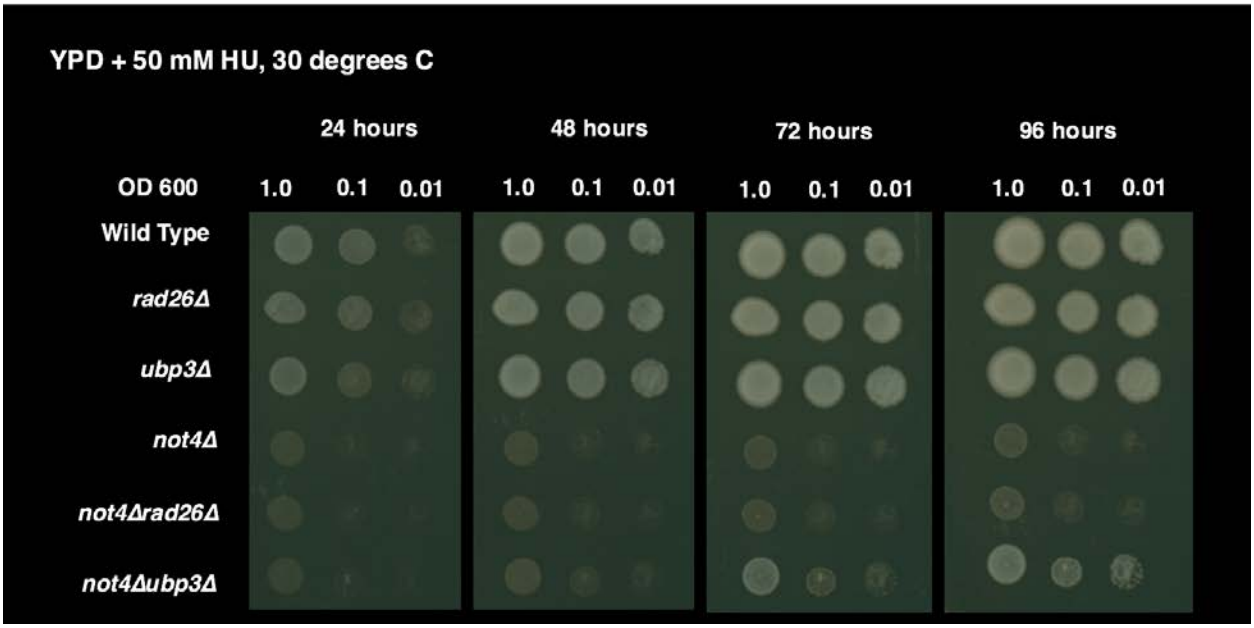

C.

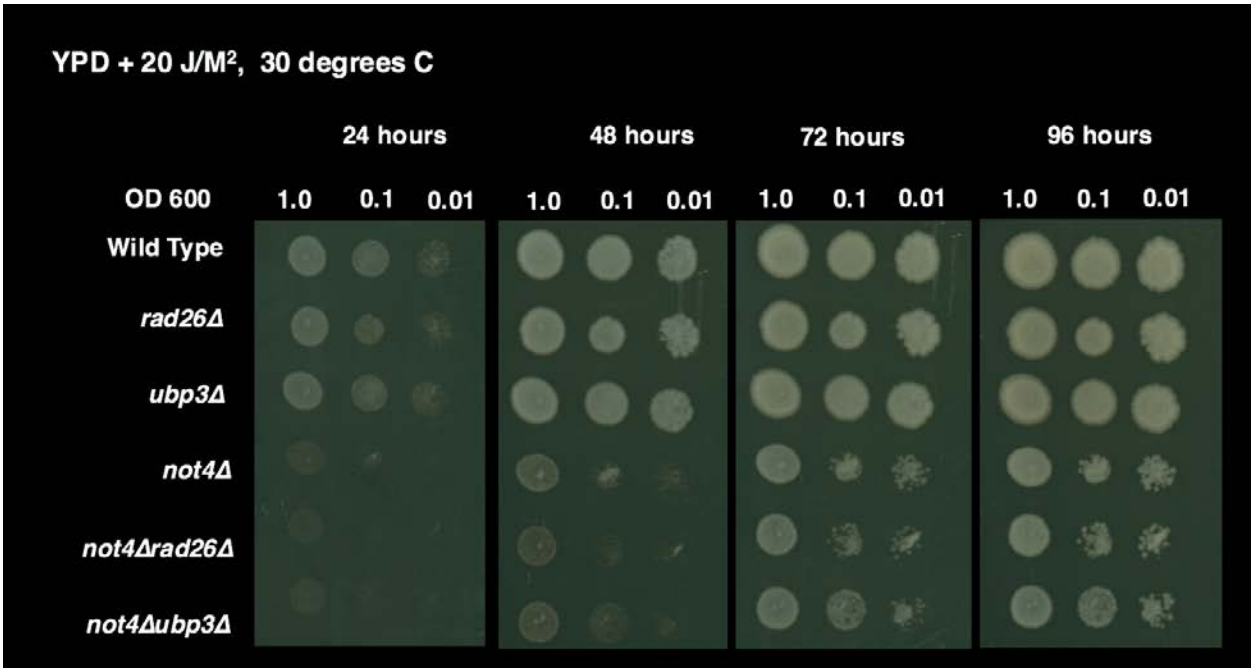
YPD + 20 J/M², 30 degrees C
24 hours
48 hours
72 hours
96 hours
OD 600
1.0 0.1 0.01
Wild Type
rad26Δ
ubp3Δ
not4Δ
not4Δrad26Δ
not4Δubp3Δ

D.

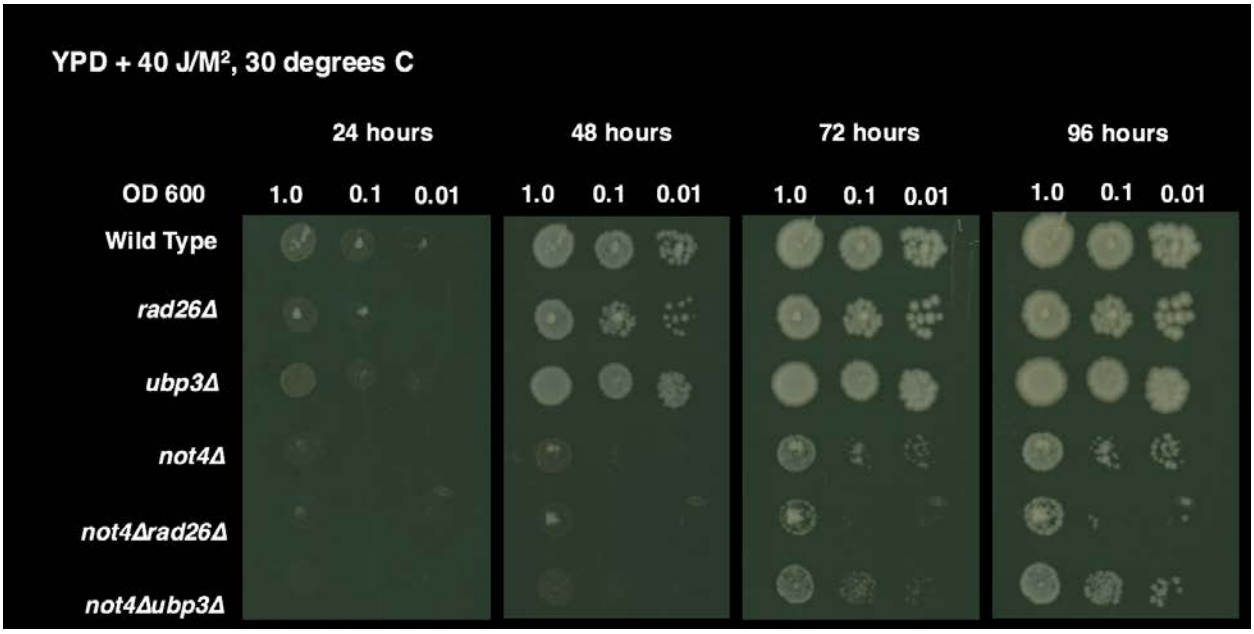
YPD + 40 J/M², 30 degrees C
24 hours
48 hours
72 hours
96 hours
OD 600
1.0 0.1 0.01
Wild Type
rad26Δ
ubp3Δ
not4Δ
not4Δrad26Δ
not4Δubp3Δ

Figure 3.7: Mutant Phenotype Response to DNA-Damaging Conditions. *not4*Δ*, rad26*Δ, and *ubp3*Δ single deletion mutants, as well as *not4*Δ*rad26*Δ and *not4*Δ*ubp3*Δ double deletion mutants, were grown and tested under control conditions (A) and a variety of stress conditions (B, C, D). The conditions tested were YPD + 25 mM hydroxyurea (HU) (30° C), YPD + 50 mM HU (30° C), YPD + 75 mM HU (30° C), YPD + 20 J/M^2 (30° C), YPD + 40 J/M^2 (30° C), YPD + 60 J/M^2 (30° C). A representative portion of tests is shown.

Figure 3.8: *not4*Δ Mutants are Temperature Sensitive

A.

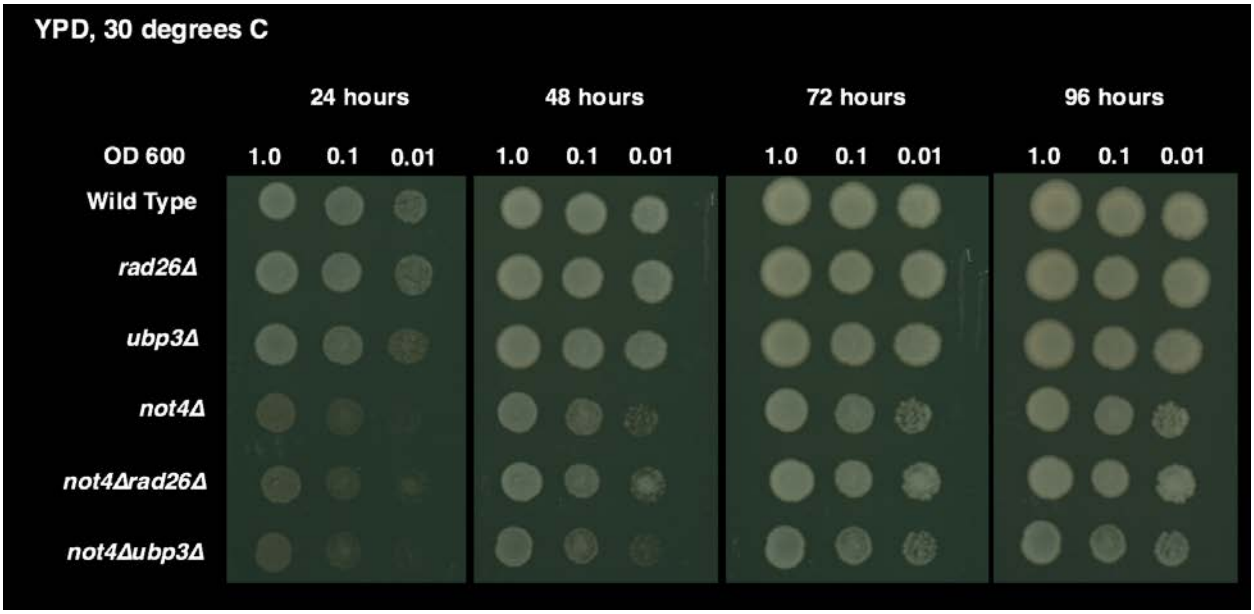

B.

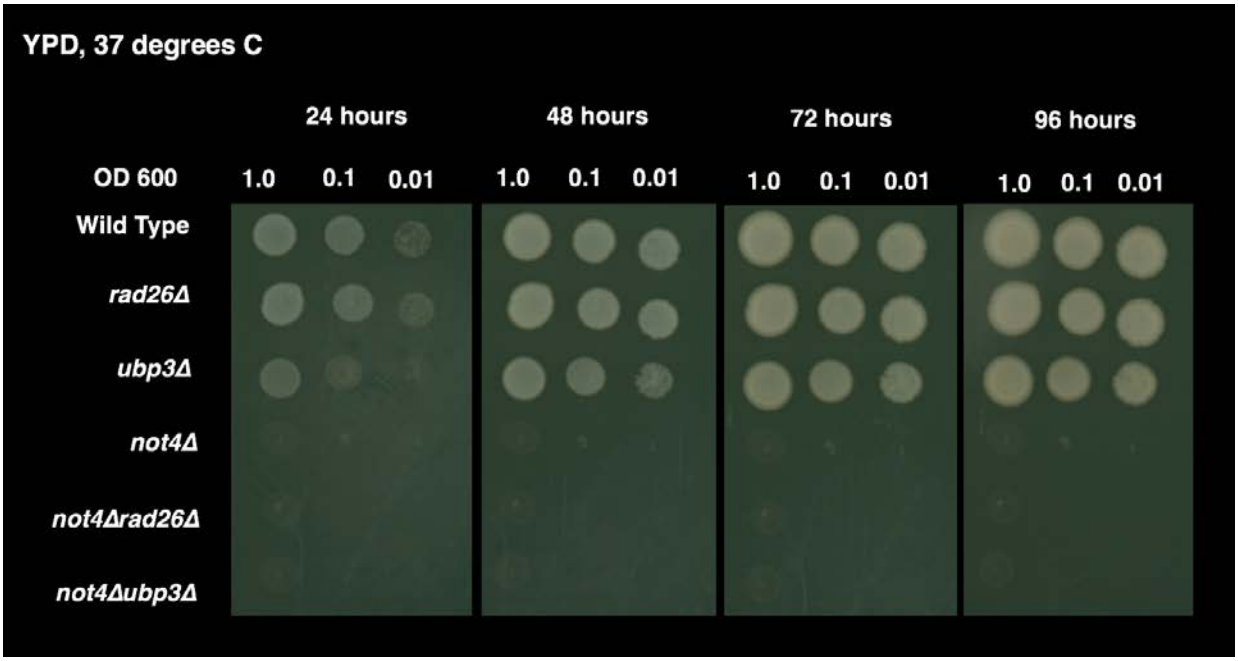

Figure 3.8: *not4*Δ Mutants are Temperature Sensitive. *not4*Δ, *rad26*Δ, and *ubp3*Δ single deletion mutants, as well as *not4*Δ*rad26*Δ and *not4*Δ*ubp3*Δ double deletion mutants were assayed for growth under control conditions (YPD at 30° C) and at higher-than-normal growth temperature (YPD at 37° C).

Figure 3.9: Mutant Survival Rates in Response to UV Radiation

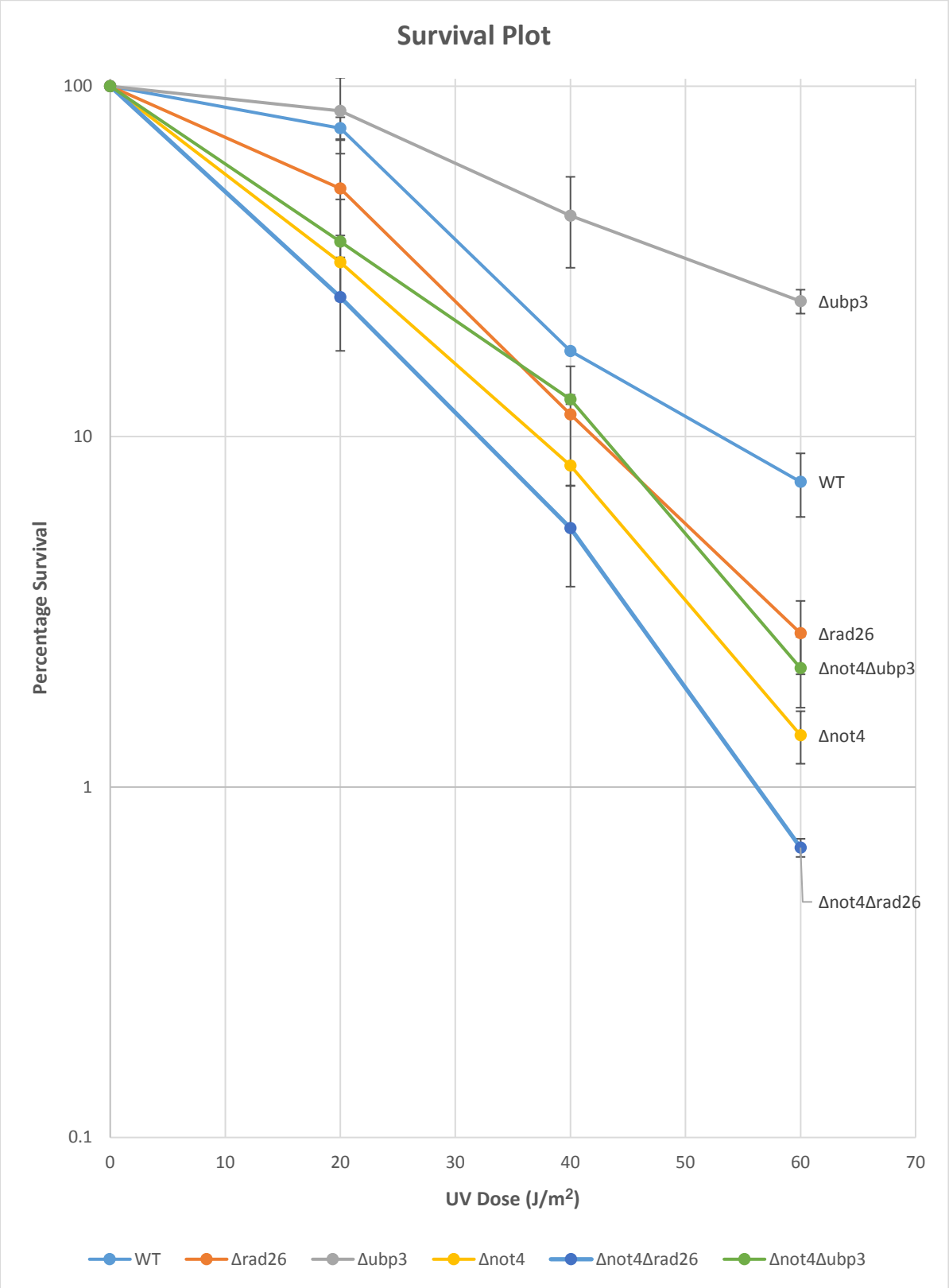

Figure 3.9: Mutant Survival Rates in Response to UV Radiation. The graph displays the UV-sensitivity of each mutant strain, quantitated using triplicate YPD plates for each tested dilution of cells and corresponding UV treatment (error bars show standard deviation among counted plates—see section 3.3). These findings were reproduced in a second, independent experiment (not shown).

Figure 3.10: The Not4 RING Domain is Important for Growth Under Stress Conditions

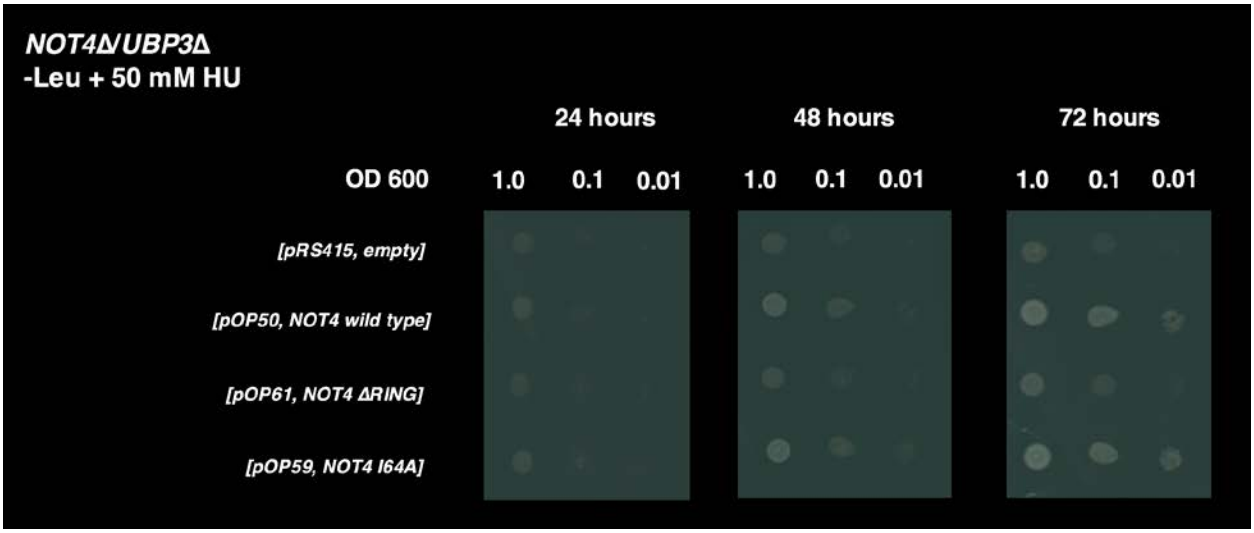

Figure 3.10: The Not4 RING Domain is Important for Growth Under Stress Conditions. Wild type, *not4*Δ, *not4*Δ*ubp3*Δ (shown), and *not4*Δ*rad26*Δ mutants were transformed with wild type and modified versions of *NOT4* on a *LEU2*-marked plasmid. The cells were grown on media containing hydroxyurea (HU), inducing stress. Restoring whole or partial RING functionality of Not4 (via the wild type plasmid or the *NOT4* I64A point mutant plasmid) rescued growth in each strain.

Figure 3.11: Mutant Rpb1 Degradation Phenotypes in Response to DNA Damage

A.

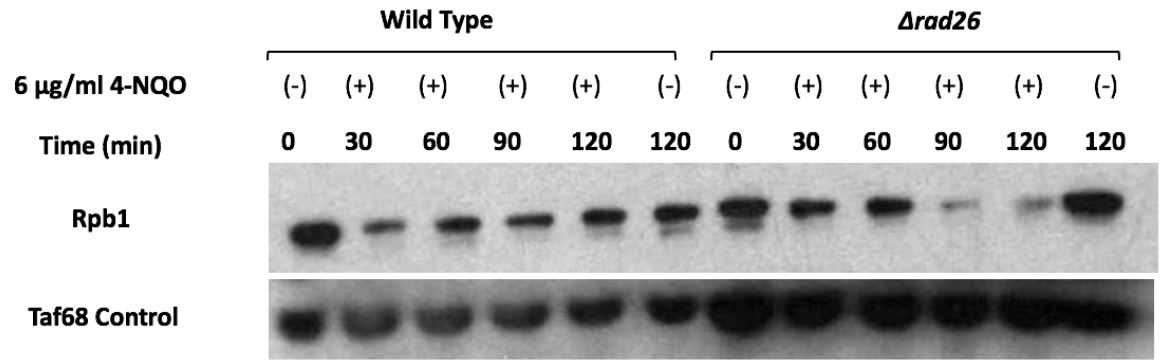

B.

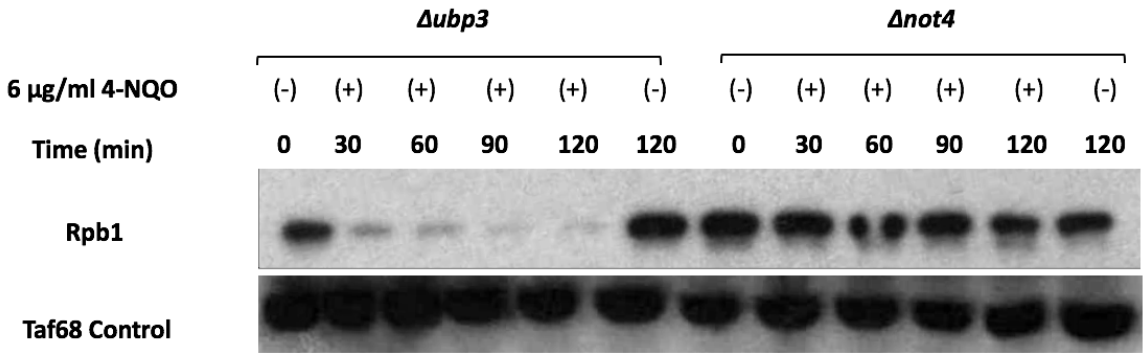

C.

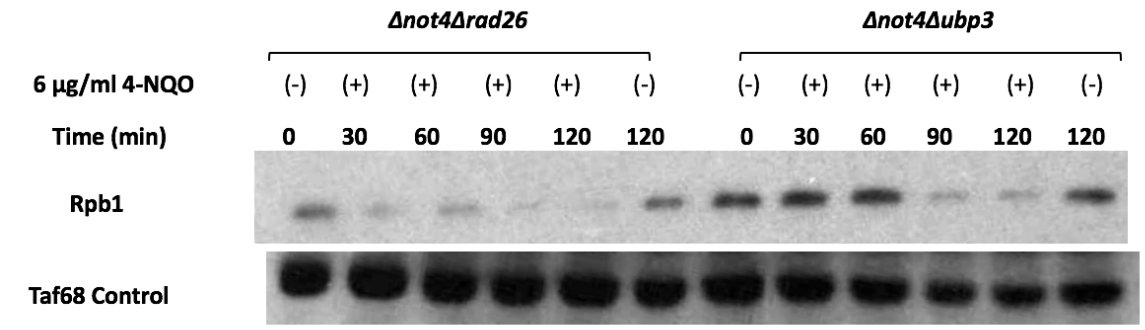
Δnot4Δrad26
Δnot4Δubp3
6 µg/ml 4-NQO
(-) (+) (+) (+) (+) (-) (-) (+) (+) (+) (+) (-)
Time (min)
0 30 60 90 120 120 0 30 60 90 120 120
Rpb1
Taf68 Control

D.

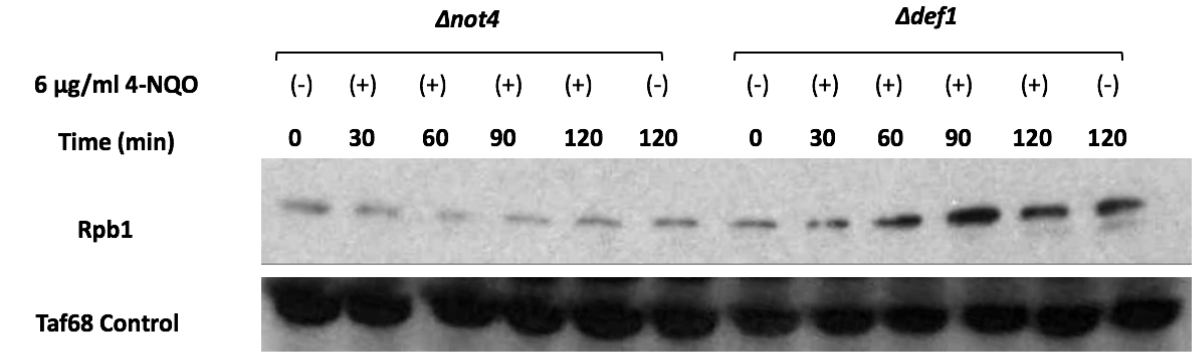
Δnot4
Δdef1
6 µg/ml 4-NQO
(-) (+) (+) (+) (+) (-) (-) (+) (+) (+) (+) (-)
Time (min)
0 30 60 90 120 120 0 30 60 90 120 120
Rpb1
Taf68 Control

E.

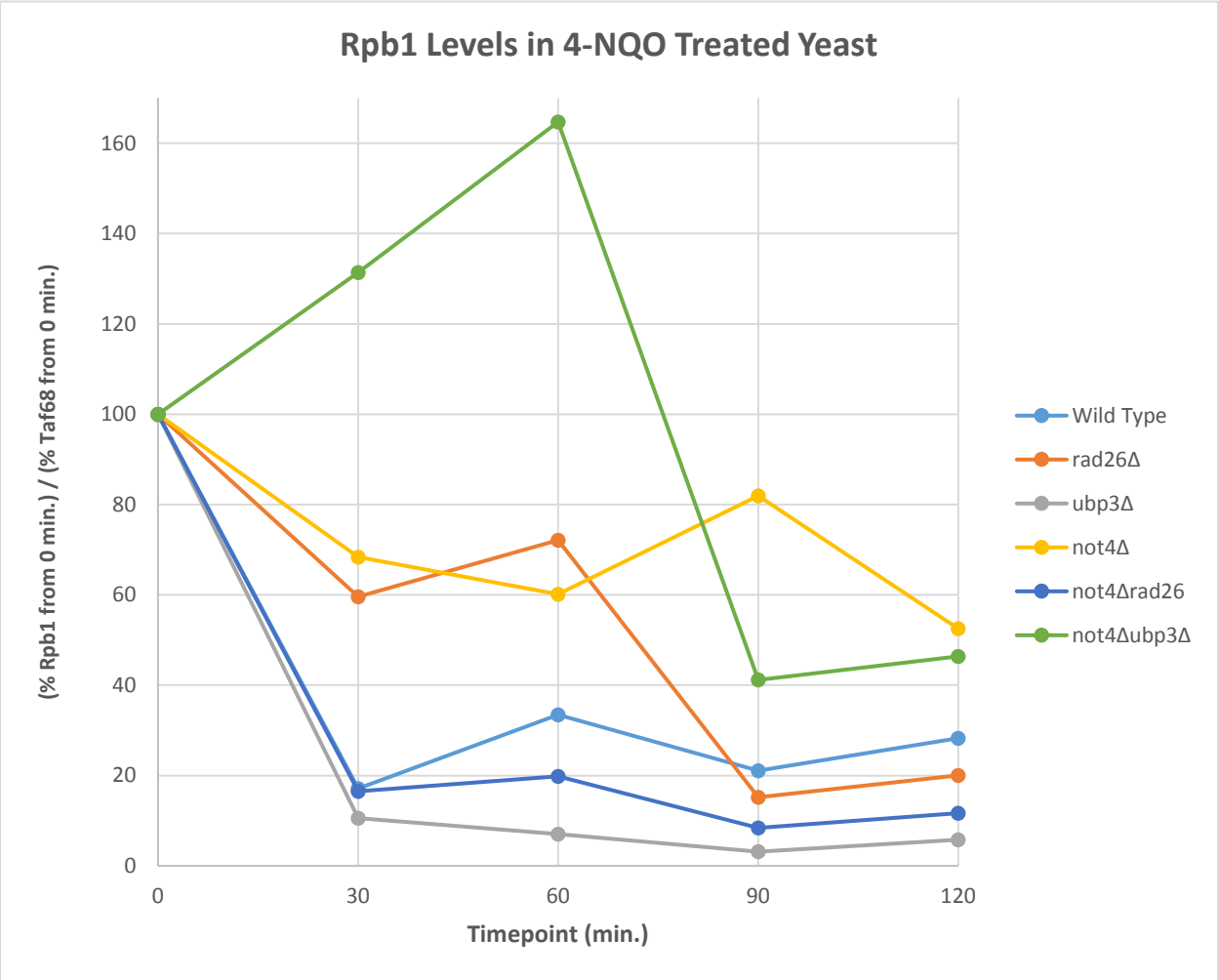

Figure 3.11: Mutant Rpb1 Degradation Phenotypes in Response to DNA Damage. Each strain was grown overnight to saturation, and then seeded in fresh YPD the next day to achieve approximately equal log phase growth among the mutants at the time of treatment. All samples were treated with 100 µg/ml cycloheximide (added at 0 minutes), and indicated samples (+) were treated with 6 µg/ml 4-NQO at the 0 minute experimental time-point. (A) Rpb1 degradation in wild type and *rad26*Δ cells. The apparent lack of smooth degradation in the wild type is likely caused by variable protein levels generated during TCA preparation. (B) Rpb1 degradation in *ubp3*Δ and *not4*Δ cells. (C) Rpb1 degradation in *not4*Δ*rad26*Δ and *not4*Δ*ubp3*Δ cells. Increases at the 30 and 60 minute time-points in the *not4*Δ*ubp3*Δ strain are likely caused by variable protein levels generated during TCA preparation. (D) *not4*Δ and *def1*Δ controls. The apparent increase in Rpb1 levels in the *def1*Δ strain is likely caused by variable protein levels generated during TCA preparation. (D) Graph of Rbp1 degradation in each experimental mutant strain. Values were generated by obtaining a density value for each band, and dividing each Rpb1 density value by the corresponding Taf68 control density value. The value for the 0-minute time-point was set to 100%, and each subsequent time-point was calculated as (Value for time-point X)/(Value for time-point 0) x 100 in order to achieve values measured as a percentage of initial Rpb1 levels.

Chapter 4

Discussion

4.1 Not4 May Act Externally to A Known Pathway for DNA Damage-Induced Polyubiquitylation and Destruction of RNAPII

The eukaryotic cell relies on a network of enzymes to resolve interruptions to transcription that can occur because of DNA damage. At the core of this response are the transcription-coupled repair (TCR) and ubiquitin/proteasome pathways. While TCR proteins are poised to repair DNA damage after RNAPII is stalled by a DNA lesion, RNAPII must first be removed from the site of damage. This may occur through backtracking, dissociation from the DNA template, or, as a last resort, degradation (47, 32, 50). However, these potential mechanisms for removal, as well as which factors may coordinate them, are not well understood. Narrowing our focus to how the "last resort" destruction of RNAPII may be regulated in *Saccharomyces cerevisiae*, integrating pathways responsible for repair and ubiquitin-mediated degradation, yields insight into how the cell navigates blocks to transcription.

The first evidence of an interdependent relationship between RNAPII degradation and DNA repair emerges from the Rad26 and Def1 proteins. Rad26 was the first eukaryotic protein found to be selectively involved in TCR, and its deletion yields viable yeast with no significant growth defect (57). This phenotype suggests that Rad26 is not directly involved in degrading RNAPII that has been stalled by DNA damage, and instead functions in some other aspect of nucleotide excision repair. Indeed, Woudstra et al. showed that Rad26 forms a complex with Def1 in chromatin, working in tandem to regulate RNAPII degradation that is instead mediated by Def1. It was found that UV-induced degradation of RNAPII in the *rad26*Δ strain occurred

more efficiently than in wild type yeast (60). (As noted in section 3.4, we also saw increased RNAPII degradation in *rad26*Δ mutants in the study conducted here.) When first discovered, this finding contradicted previous beliefs that RNAPII degradation was itself sufficient for TCR, since *rad26*Δ cells are greatly TCR-compromised (31). At the same time, *def1*Δ mutants did not degrade RNAPII at all, but simultaneous deletion of *RAD26* reactivated RNAPII degradation in the *def1*Δ*rad26*Δ strain. Def1 and Rad26 do not require each other for function, despite forming a complex—just as cells lacking Rad26 are adept in degrading RNAPII, cells lacking Def1 can repair lesions in the transcribed strand of active genes. However, Def1 is critically necessary for damage-induced RNAPII degradation when Rad26 is present; in the absence of Rad26, the safeguard protecting RNAPII from degradation is removed (60).

Def1-mediated degradation of RNAPII after DNA damage has been shown to occur via the polyubiquitylation of Rpb1, the large subunit of RNAPII. In order to initiate degradation, Def1 must undergo proteasomal processing that results in its transport to the nucleus and binding to RNAPII. This occurs when Rsp5, an E3 ubiquitin ligase, monoubiqitylates Def1 in response to intracellular stress signals. After binding RNAPII, Def1 helps to recruit Elc1/Cul3, the Elongin-Cullin complex, via a ubiquitin homology domain. Elc1/Cul3 then polyubiquitylates Rpb1, promoting its proteasomal-mediated degradation. (59)

It has been previously shown in the Reese laboratory that the Not4 RING domain is also heavily implicated in Rpb1 degradation during DNA-damaging conditions (30). The observation that Rpb1 turnover is impaired after DNA damage in *not4*Δ mutants was reiterated here. Taken together with findings that the Ccr4-Not complex interacts directly with stalled RNAPII during elongation (11), there is compelling evidence that ubiquitylation by Not4 provides the cell with another means of regulating Rpb1 destruction during transcriptional arrest. RNAPII must be

removed from a damaged gene to initiate repair, making degradation a sometimes-necessary outcome. However, degrading RNAPII places a high energetic cost on the cell and only occurs as a "last resort" response. Therefore, the potential existence of multiple, conserved pathways designed to regulate this decision is justified.

In this study, the first evidence that Not4 may act in a pathway parallel to Def1 and Elc1/Cul3 comes from the existence of a synthetically lethal interaction between Def1 and Not4. Synthetic (or epistatic) interactions are defined by the presence of a double mutant phenotype that differs from either single mutant "parent" phenotype. Synthetically lethality is the opposite of suppression—the double mutants are inviable, even when individual single mutants are viable. (In contrast, synthetically viable mutants, or suppressors, are viable even when at least one of the single mutants is not.) The lethal interaction signifies a possible pathway redundancy; in effect, the cell retains several modes of achieving the same outcome.(12) Here, the activities of Def1 and Not4 may both converge on the eventual polyubiquitylation and degradation of RNAPII. Specifically, the Not4 RING domain—conferring ubiquitylation activity—is necessary to restore double mutant growth.

The viability of *not4*Δ*rad26*Δ mutants allows for a more nuanced investigation into the genetic interactions of these perhaps disparate pathways. Testing the survival rate of the *not4*Δ*rad26*Δ strain under UV radiation revealed that these double mutants are more UV-sensitive than the parent *not4*Δ single mutant, again signaling possible epistasis. Interestingly, Rpb1 appears to be degraded at a higher rate in *not4*Δ*rad26*Δ mutants than in *not4*Δ mutants during DNA damage. Although this result needs to be repeated and verified, it fits well in relation to current knowledge about the relationship between Def1 and Rad26. In the single *not4*Δ mutant, Rad26 is present to exert a protective effect on RNAPII. When *RAD26* is deleted,

however, it may permit increased Def1-mediated degradation of Rpb1. Further study of *not4*Δ mutants, in conjunction with simultaneous deletions in the Elc1/Cul3 degradation pathway, will yield more insight about where the activity of these enzymes converges.

4.2 The Relationship of Not4 with Ubiquitin Proteases Acting on DNA Damage-Stalled RNAPII

While RNAPII undergoes polyubiquitylation during DNA damage, the cell also retains a mode of deubiquitylating RNAPII via the Ubp3 ubiquitin protease. Kvint et al. uncovered this important regulatory role for Ubp3 when it was observed that the enzyme copurifies with RNAPII, Def1, and the elongation factors Spt5 and TFIIF, and Ubp3 deubiquitylates mono- and polyubiquitylated RNAPII *in vitro*. Critically, *ubp3*Δ cells were also shown to have higher levels of *in vivo* ubiquitylated RNAPII, which caused RNAPII to undergo proteasome-mediated degradation more rapidly in response to DNA damage. (28) Ubp3 thus provides the cell with a means of reversing the "decision" to degrade polymerase, affording more time to repair DNA damage and rescue transcription.

Our studies of *ubp3*Δ single mutants reproduce the results of Kvint et al. We showed that under DNA-damaging conditions, Rpb1 is degraded more quickly by *ubp3*Δ mutants than wild type cells. In the UV survival assay, *ubp3*Δ mutants were also less sensitive than wild type yeast to increases in UV radiation. This is consistent with the idea that increased RNAPII degradation acts to suppress DNA repair defects. It has also been shown, for example, that *ubp3*Δ*rad26*Δ double mutants, in which TCR is compromised, are less sensitive to UV radiation than *rad26*Δ single mutants (28).

Because we have repeatedly shown the ubiquitylation activity of Not4 to be a critical regulator of RNAPII degradation during DNA damage, it is important to understand its activity in context with Ubp3. Spot assays showed that in the presence of hydroxyurea or DNA damage-inducing UV light, *not4*Δ*ubp3*Δ double mutants have a stronger growth rate than *not4*Δ single mutants. These findings were complemented in finer detail by the observation that *not4*Δ*ubp3*Δ cells have a quantitatively higher survival rate than the *not4*Δ strain during UV irradiation. Increased capacity for survival suggested that degradation of RNAPII may not be as impaired in the *not4*Δ*ubp3*Δ double mutant strain as in *not4*Δ mutants, highlighting the previously observed protective effect of *UBP3* deletion on DNA damage repair defects. Indeed, we found that Rpb1 degradation is accelerated in *not4*Δ*ubp3*Δ mutants when compared to *not4*Δ mutants, though not to the same extent as in *not4*Δ*rad26*Δ mutants. As described previously, this could be a result of Rad26 operating to partially inhibit the action of Def1-mediated RNAPII degradation. An important future experiment would be to verify that the effect of Not4 RING deletion on these results remains the same as total Not4 deletion. Additional future studies of Rpb1 polyubiquitylation *in vitro*, performed on combinations of mutations in *NOT4*, *UBP3*, and the *ELC1/CUL3* pathway would also help to illuminate how, and to what extent, RNAPII degradation is regulated by various competing forces.

4.3 Summary and Outlook

Previous studies have implicated Ccr4-Not in general (56), and the E3 ubiquitin ligase activity of Not4 specifically (30), in the budding yeast DNA damage response. Here, we verified that Not4 plays an important role in RNAPII degradation during DNA damage, as seen in the

lack of Rpb1 degradation among *not4*Δ mutants subjected to DNA-damaging conditions. We also investigated the genetic interactions of *NOT4* with other known facilitators of the TCR response in yeast. From observed epistatic interactions between *NOT4* and the *RAD26/DEF1* complex, we conclude that Not4 may act externally to a known pathway mediating the polyubiquitylation and destruction of Rpb1, caused by Elc1/Cul3 (Figure 4.1). Additionally, Not4 does not appear to be strictly necessary for the polyubiquitylation of Rpb1, as seen in the accelerated degradation of Rpb1 among *not4*Δ*ubp3*Δ and *not4*Δ*rad26*Δ mutants during DNA-damaging conditions. It remains to be seen whether Not4 directly ubiquitylates RNAPII, or if it promotes Rpb1 degradation in another manner, perhaps by ubiquitylating some adaptor protein.

Understanding the DNA damage repair pathway in eukaryotes, of which Ccr4-Not is a critical part, will allow scientists to address its alterations. Better comprehension can ultimately lead to the prevention and treatment of ailments caused by accumulated mutations. Defects in TCR have been specifically linked to multiple hereditary diseases in humans, and DNA damage in general has been shown to both upset cellular homeostasis and cause premature cell death. By learning in detail how the cell repairs DNA lesions, researchers will be better equipped to resolve pathologies—such as cancer and aging—that manifest after affronts to DNA integrity.

Figure 4.1: Potential Models of Ccr4-Not Action During RNAPII Degradation in Response to DNA Damage

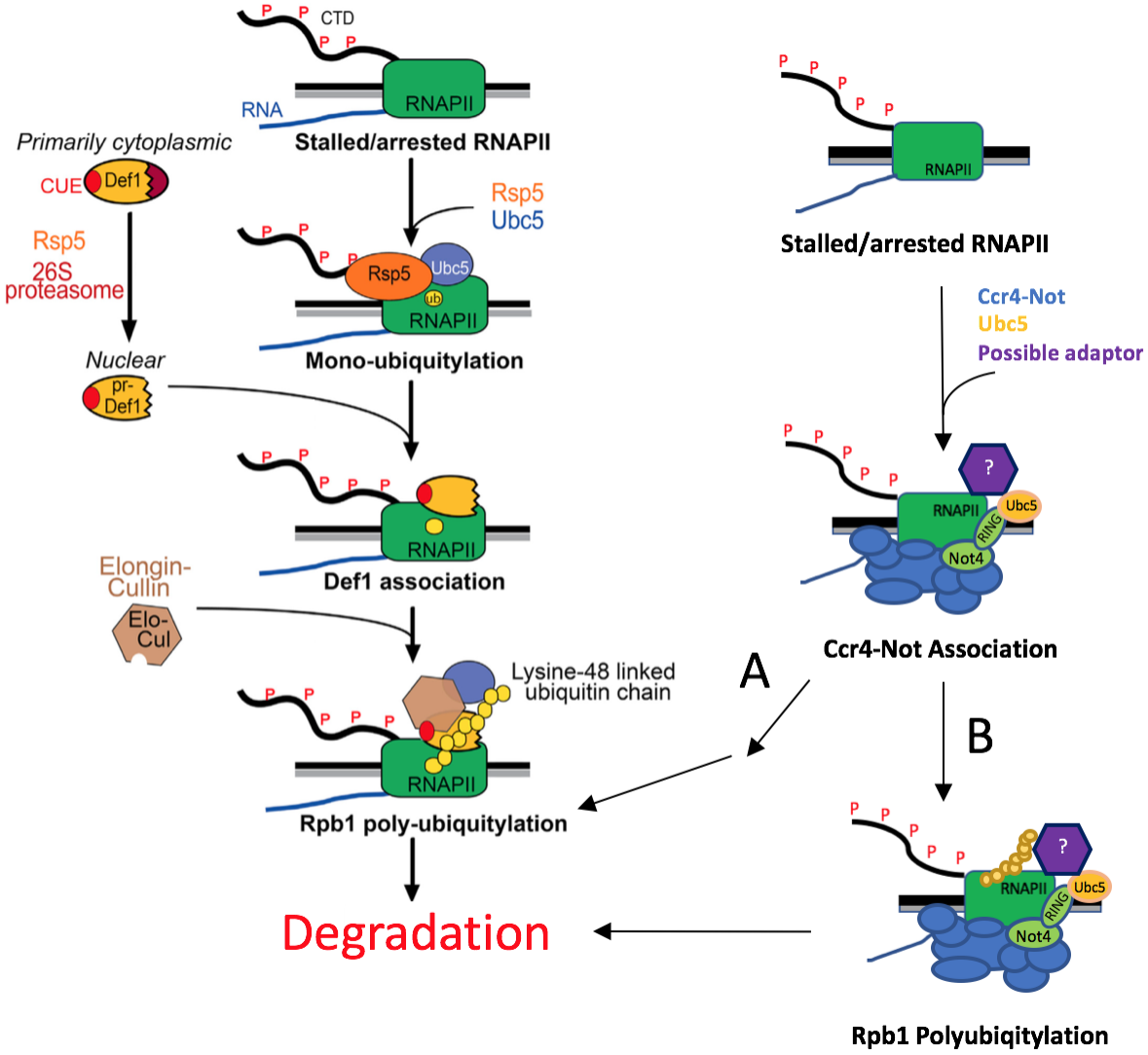

Figure 4.1: Potential Models of Ccr4-Not Action During RNAPII Degradation in Response to DNA Damage. Adapted from (59). Ccr4-Not may act externally to the known Def1-mediated pathway for DNA damage-induced polyubiquitylation and destruction of RNAPII. As seen in (A), Ccr4-Not could recruit Elc1/Cul3 by other means, perhaps by either directly ubiquitylating Rpb1 or ubiquitylating some adaptor protein. Or, as in (B), Ccr4-Not could trigger polyubiquitylation without Elc1/Cul3.

BIBLIOGRAPHY

1. Alberts B, Johnson A, Lewis J, et al. Molecular Biology of the Cell. 4th edition. New York: Garland Science; 2002. DNA Repair.

2. Bilsland, E., Hult, M., Bell, S. D., Sunnerhagen, P. & Downs, J. A. The Bre5/Ubp3 ubiquitin protease complex from budding yeast contributes to the cellular response to DNA damage. *DNA Repair (Amst).* **6,** 1471–1484 (2007).

3. Boeke, J. D., Trueheart, J., Natsoulis, G. & Fink, G. R. [10] 5-Fluoroorotic acid as a selective agent in yeast molecular genetics. *Methods Enzymol.* **154,** 164–175 (1987).

4. Boiteux, S. & Jinks-Robertson, S. DNA repair mechanisms and the bypass of DNA damage in Saccharomyces cerevisiae. *Genetics* **193,** 1025–1064 (2013).

5. Brachmann, C. B. *et al.* Designer deletion strains derived from Saccharomyces cerevisiae S288C: A useful set of strains and plasmids for PCR-mediated gene disruption and other applications. *Yeast* **14,** 115–132 (1998).

6. Collart, M. A. & Panasenko, O. O. The Ccr4-Not complex. *Gene* **492,** 42–53 (2012).

7. Collart, M. A. & Struhl, K. NOT1(CDC39), NOT2(CDC36), NOT3, and NOT4 encode a global-negative regulator of transcription that differentially affects TATA-element utilization. *Genes Dev.* **8,** 525–537 (1994).

8. Cooper, K. F. *et al.* Oxidative-stress-induced nuclear to cytoplasmic relocalization is required for Not4-dependent cyclin C destruction. *J. Cell Sci.* **125,** 1015–1026 (2012).

9. Cramer, P. Architecture of RNA Polymerase II and Implications for the Transcription Mechanism. *Science (80-.).* **288,** 640–649 (2000).

10. Cramer, P. *et al.* Transcription : RNA Polymerase. **292,** 1863–1876 (2017).

11. Dutta, A. *et al.* Ccr4-Not and TFIIS Function Cooperatively To Rescue Arrested RNA Polymerase II. TL - 35. *Mol. Cell. Biol.* **35,** 1915–1925 (2015).

12. Forsburg, S. The art and design of genetic screens: yeast. *Nat Rev Genet* **2,** 956–966 (2001).

13. Gates, K. S. An overview of chemical processes that damage cellular DNA: Spontaneous hydrolysis, alkylation, and reactions with radicals. *Chem. Res. Toxicol.* **22,** 1747–1760 (2009).

14. Gulshan, K., Thommandru, B. & Moye-Rowley, W. S. Proteolytic degradation of the Yap1 transcription factor is regulated by subcellular localization and the E3 ubiquitin ligase Not4. *J. Biol. Chem.* **287,** 26796–26805 (2012).

15. Halter, D., Collart, M. A. & Panasenko, O. O. The Not4 E3 ligase and CCR4 deadenylase play distinct roles in protein quality control. *PLoS One* **9,** (2014).

16. Hanawalt, P. C. & Spivak, G. Transcription-coupled DNA repair: two decades of progress and surprises. *Nat. Rev. Mol. Cell Biol.* **9,** 958–70 (2008).

17. Hardesty, B. The Mechanism by which Cycloheximide Glutarimide Antibiotics Inhibit Peptide Synthesis on Reticulocyte Ribosomes *. (1971).

18. Harreman, M. *et al.* Distinct ubiquitin ligases act sequentially for RNA polymerase II polyubiquitylation. *Proc. Natl. Acad. Sci. U. S. A.* **106,** 20705–20710 (2009).

19. Hershko, A. & Ciechanover, A. The ubiquitin system. *Annu. Rev. Biochem.* **67,** 425–479 (1998).

20. Herskowitz, I. Life cycle of the budding yeast Saccharomyces cerevisiae. *Microbiol. Rev.* **52,** 536–553 (1988).

21. Ikenaga, M., Ichikawa-Ryo, H. & Kondo, S. The major cause of inactivation and mutation by 4-Nitroquinoline 1-Oxide in Escherichia coli: Excisable 4NQO-purine adducts. *J. Mol. Biol.* **92,** 341–356 (1975).

22. Karakasili, E., Burkert-Kautzsch, C., Kieser, A. & Sträßer, K. Degradation of DNA damage-independently stalled RNA polymerase II is independent of the E3 ligase Elc1. *Nucleic Acids Res.* **42,** 10503–10515 (2014).

23. Kelner, A. (1949). Effect of Visible Light on the Recovery of Streptomyces Griseus Conidia from Ultra-violet Irradiation Injury. *Proceedings of the National Academy of Sciences of the United States of America, 35*(2), 73–79.

24. Kim, B. *et al.* The transcription elongation factor TFIIS is a component of RNA polymerase II preinitiation complexes. *Proc. Natl. Acad. Sci. U. S. A.* **104,** 16068–16073 (2007).

25. Kireeva, M., Kashlev, M. & Burton, Z. F. Translocation by multi-subunit RNA polymerases. *Biochim. Biophys. Acta - Gene Regul. Mech.* **1799,** 389–401 (2010).

26. Koç, A., Wheeler, L. J., Mathews, C. K. & Merrill, G. F. Hydroxyurea Arrests DNA Replication by a Mechanism that Preserves Basal dNTP Pools. *J. Biol. Chem.* **279,** 223–230 (2004).

27. Kruk, J. A. *et al.* transcription elongation The multifunctional Ccr4 – Not complex directly promotes transcription elongation. 581–593 (2011).

28. Kvint, K. *et al.* Reversal of RNA Polymerase II Ubiquitylation by the Ubiquitin Protease Ubp3. *Mol. Cell* **30,** 498–506 (2008).

29. Li, K., Ossareh-Nazari, B., Liu, X., Dargemont, C. & Marmorstein, R. Molecular Basis for Bre5 Cofactor Recognition by the Ubp3 Deubiquitylating Enzyme. *J. Mol. Biol.* **372,** 194–204 (2007).

30. Libert, D. (2014). A Genetic and Biochemical Analysis of the Role of the Ccr4-Not Complex in Transcription Elongation and Recovery form DNA Damage in Budding Yeast. Honors Thesis, Penn State Dept. of Biochemistry and Molecular Biology.

31. Lommel, L., Bucheli, M. & Sweder, K. Transcription-coupled repair in yeast is independent from ubiquitylation of RNA pol II: implications for Cockayne's syndrome. *Proc. Natl. Acad. Sci. U. S. A.* **97,** 9088–9092 (2000).

32. Marteijn, J. a, Lans, H., Vermeulen, W. & Hoeijmakers, J. H. J. Understanding nucleotide excision repair and its roles in cancer and ageing. *Nat. Rev. Mol. Cell Biol.* **15,** 465–81 (2014).

33. Martinez-Rucobo, F. W. & Cramer, P. Structural basis of transcription elongation. *Biochim Biophys Acta* **1829,** 9–19 (2013).

34. Mersman, D. P., Du, H. N., Fingerman, I. M., South, P. F. & Briggs, S. D. Polyubiquitination of the demethylase Jhd2 controls histone methylation and gene expression. *Genes Dev.* **23,** 951–962 (2009).

35. Miller, J. E. & Reese, J. C. Ccr4-Not complex: the control freak of eukaryotic cells. *Crit. Rev. Biochem. Mol. Biol.* **47,** 315–333 (2012).

36. Min, J. H., and N. P. Pavletich, 2007 Recognition of DNA damage by the Rad4 nucleotide excision repair protein. Nature 449: 570–575.

37. Mulder, K. W. *et al.* Modulation of Ubc4p/Ubc5p-mediated stress responses by the RING-finger-dependent ubiquitin-protein ligase Not4p in Saccharomyces cerevisiae. *Genetics* **176,** 181–192 (2007).

38. Ohkuni K, Kikuchi Y, Hara K, Taneda T, Hayashi N, Kikuchi A. (2006). Suppressor analysis of the mpt5/htr1/uth4/puf5 deletion in *Saccharomyces cerevisiae*. *Mol Genet Genomics* 275, 81–88.

39. Olesya, O., Panasenko, O. & Collart, M. A. Not4 E3 Ligase Contributes to Proteasome Assembly and Functional Integrity in Part through Ecm29. *Mol. Cell. Biol.* **31,** 1610–1623 (2011).

40. Park, J. S. & Roberts, J. W. (2006). Role of DNA bubble rewinding in enzymatic transcription termination. *Proc. Natl Acad. Sci. USA* 103, 4870–4875.

41. Reese, J. C. The control of elongation by the yeast Ccr4-Not complex. *Biochim. Biophys. Acta - Gene Regul. Mech.* **1829,** 127–133 (2013).

42. Ribar, B., Prakash, L. & Prakash, S. Requirement of ELC1 for RNA polymerase II polyubiquitylation and degradation in response to DNA damage in Saccharomyces cerevisiae. *Mol. Cell. Biol.* **26,** 3999–4005 (2006).

43. Rupert, C. S. (1962). Photoenzymatic Repair of Ultraviolet Damage in DNA : I. *Kinetics of the reaction*. *The Journal of General Physiology*, *45*(4), 703–724.

44. Sancar, A. Mechanism of DNA excision repair. *Science (80-.).* **266,** 1954–1956 (1994).

45. Saunders, A., Core, L. & Lis, J. Breaking barriers to transcription elongation. *Nat Rev Mol Cell Biol* **7,** 557–567 (2006).

46. Shilatifard, A., Conaway, R. C. & Conaway, J. W. The RNA Polymerase II Elongation Complex. *Annu. Rev. Biochem.* **73,** 293–320 (2004).

47. Sigurdsson, S., Dirac-Svejstrup, A. B. & Svejstrup, J. Q. (2010). Evidence that transcript cleavage is essential for RNA polymerase II transcription and cell viability. *Mol. Cell* 38, 202–210.

48. Somesh, B. P. *et al.* Multiple mechanisms confining RNA polymerase II ubiquitylation to polymerases undergoing transcriptional arrest. *Cell* **121,** 913–923 (2005).

49. Somesh, B. P. *et al.* Communication between Distant Sites in RNA Polymerase II through Ubiquitylation Factors and the Polymerase CTD. *Cell* **129,** 57–68 (2007).

50. Svejstrup, J. Q. Contending with transcriptional arrest during RNAPII transcript elongation. *Trends Biochem. Sci.* **32,** 165–171 (2007).

51. Swenberg, J. A. *et al.* Endogenous versus exogenous DNA adducts: Their role in carcinogenesis, epidemiology, and risk assessment. *Toxicol. Sci.* **120,** 130–145 (2011).

52. Sydow, J. F. *et al.* Structural Basis of Transcription: Mismatch-Specific Fidelity Mechanisms and Paused RNA Polymerase II with Frayed RNA. *Mol. Cell* **34,** 710–721 (2009).

53. Sydow, J. F. & Cramer, P. RNA polymerase fidelity and transcriptional proofreading. *Curr. Opin. Struct. Biol.* **19,** 732–739 (2009).

54. Thomas, M. J., Platas, A. A. & Hawley, D. K. Transcriptional fidelity and proofreading by RNA polymerase II. *Cell* **93,** 627–637 (1998).

55. Tornaletti, S., Reines, D. & Hanawalt, P. C. (1999). Structural characterization of RNA polymerase II complexes arrested by a cyclobutane pyrimidine dimer in the transcribed strand of template DNA. *J. Biol. Chem.* 274, 24124–24130.

56. Traven, A., Hammet, A., Tenis, N., Denis, C. L. & Heierhorst, J. Ccr4-not complex mRNA deadenylase activity contributes to DNA damage responses in Saccharomyces cerevisiae. *Genetics* **169,** 65–75 (2005).

57. van Gool, A. J. *et al.* RAD26, the functional S. cerevisiae homolog of the Cockayne syndrome B gene ERCC6. *EMBO J.* **13,** 5361–9 (1994).

58. Westover, K. D., Bushnell, D. A. & Kornberg, R. D. Structural basis of transcription: Nucleotide selection by rotation in the RNA polymerase II active center. *Cell* **119,** 481–489 (2004).

59. Wilson, M. D. *et al.* Proteasome-mediated processing of Def1, a critical step in the cellular response to transcription stress. *Cell* **154,** 983–995 (2013).

60. Woudstra, E. C. *et al.* A Rad26-Def1 complex coordinates repair and RNA pol II proteolysis in response to DNA damage. TL - 415. *Nature* **415,** 929–933 (2002).

ACADEMIC VITA

Laura Beebe
lmbeebe@gmail.com

EDUCATION

The Pennsylvania State University, University Park, PA 16802 2013-2017
B.Sc. In Biochemistry and Molecular Biology, Mathematics (Minor)
Schreyer Honors College

RESEARCH EXPERIENCE

Honors Thesis Work: Center for Eukaryotic Gene Regulation Fall 2013-Present
Penn State University, University Park, PA: Dept. of Biochemistry and Molecular Biology
Principal Investigator: Prof. Joseph Reese
Analysis of genetic interactions between subunits of the Ccr4-Not gene regulatory complex and the ubiquitin/proteasome pathway in budding yeast (*Saccharomyces cerevisiae).*

- Isolated and verified yeast mutants via PCR KO and screening
- Dissected yeast asci to generate double mutants
- Analyzed mutant DNA damage phenotypes with growth assays and western blotting

Summer Research Intern: Developmental Neuroscience Summer 2016
Thomas Jefferson University, Philadelphia, PA: Dept. of Neuroscience
Principal Investigator: Prof. Le Ma
Analysis of cerebellar Purkinje cell branching morphogenesis after targeted cell injury or CRISPR-mediated gene knockout in mice.

- Delivered mouse viral injections and prepared brain tissue samples
- Immunohistochemically labeled Purkinje cells and took images with confocal microscopy
- Analyzed cell phenotypes with ImageJ and Neurolucida

Team Member: Penn State iGEM Spring 2015-Fall 2015
Penn State University, University Park, PA: Dept. of Chemical Engineering
Principal Investigator: Prof. Costas Maranas
Project in collaboration with students at the Washington University in St. Louis to optimize nitrogen fixation in *E. coli* via a systems biology approach. Received Bronze Award at the Fall 2015 International Genetically Engineered Machine (iGEM) competition in Boston, MA. Supported by NSF Grant No. 1331194.

- Performed flux balance analysis and flux variability analysis using Python and GAMS (General Algebraic Modeling System)
- Developed a command workflow to systematically assess all single and double gene knockouts in a genome-scale metabolic reconstruction
- Identified genetic interventions *in silico* to facilitate optimal nitrogenase activity in *E. coli*

PRESENTATIONS

Penn State Undergraduate Research Symposium Spring 2015, Spring 2016, Fall 2016
University Park, PA
Poster presentation: "Analysis of genetic interactions between subunits of the Ccr4-Not complex and the ubiquitin/proteasome pathway in budding yeast"

Thomas Jefferson University Summer 2016
Philadelphia, PA
Oral presentation: "Characterization of targeted injury model in mouse cerebellar Purkinje cells"

International Genetically Engineered Machine (iGEM) Competition Fall 2015
Boston, MA
Oral and poster presentation: "Construction of a minimal *nif* gene cluster and computational modeling to optimize nitrogen fixation in *E. coli*". Received Bronze Award.

RELEVANT COURSE PROJECTS

RNAi Screening in *Drosophila* Sensory Neurons Fall 2016
BMB 448

- Expressed hairpin RNA to knock down candidate gene in ddaE sensory neurons
- Took live images of fluorescent neurons in *Drosophila* larvae and processed in Photoshop/ImageJ
- Assessed dendrite morphology and organelle localization phenotype via statistical t-test

Isolation and Purification of *Pseudanabaena* Phycobiliproteins Fall 2015
BMB 442

- Separated phycobiliprotein standard complexes with ion exchange chromatography
- Purified proteins using salt fractionation, centrifugation, and dialysis
- Analyzed purified subunits using SDS-PAGE

Multistep Organic Synthesis of Chrysanthemic Acid (Honors Team Project) Spring 2015
CHEM 213H

- Synthesized *trans*-chrysanthemic acid, a natural insecticide, from 3-methyl-2-butenoic acid and 2-methyl-3-buten-2-ol
- Nine step organic synthesis; main techniques included refluxing with condenser, ether extractions, rotary evaporation, recrystallization, column chromatography, ^{1}H NMR, ^{13}C NMR
- Presented results at a poster session for Penn State Chemistry Dept. faculty, awarded 1st place poster out of ~10 competing

INTERNATIONAL COURSEWORK

Cellular and Reproductive Biology Summer Program in Shanghai Summer 2014
Fudan University, Shanghai, China
One of eight participants in a five-week dual-course molecular biology program in Shanghai. Funding provided by Penn State ECoS Science Travel Grant, Schreyer Honors College Travel Grant, and Fudan University.

LEADERSHIP/TEACHING

Learning Assistant *Penn State University, University Park, PA*
BMB 401 (General Biochemistry I) Fall 2016

- Led weekly problem solving sessions (~40 students per session)
- Helped students with in-class i-Clicker questions

BMB 251 (Molecular and Cellular Biology I) Spring 2015

- Led weekly problem solving sessions (~20 students per session)
- Trained in pedagogy for science education

Penn State Biochemistry Society, President Fall 2016- Spring 2017

- Coordinated research and career talks, science outreach opportunities, and social events for undergraduate club
  (25 active members)

Penn State Student Programming Association, Distinguished Lectures Committee Fall 2015- Fall 2016

- Fifteen-member committee responsible for allocating a $200k budget in order to bring distinguished speakers to the Penn State University Park campus, open and free of charge to all students

Science LionPride, General Member Fall 2013 – Fall 2016

- Application-based service and outreach group of the Penn State Eberly College of Science
- Led tours of the College of Science for prospective students and their families

HONORS/AWARDS:

- Penn State Eberly College of Science Braddock Scholarship (1 of 12 given per class) 2013-2017
- Schreyer Honors College Academic Excellence Scholarship 2013-2017
- Penn State Eberly College of Science Undergraduate Research Award 2015
- Penn State Provost Award 2013

PROGRAMMING/TECHNICAL SKILLS:

- **Proficient:** Python, C++, GAMS, NIH ImageJ, Neurolucida, Adobe Photoshop, Imaris
- **Familiar:** MATLAB, R, Minitab (Statistics)

OTHER ACTIVITIES

- Nittany Grotto Caving Club Spring 2015, Fall 2016
- Penn State Tea Institute Spring 2015- Fall 2015
- The GLOBE Honors Special Living Option Fall 2013- Spring 2014